

## Article

# A Tumor-Specific Molecular Network Promotes Tumor Growth in *Drosophila* by Enforcing a Jun N-Terminal Kinase–Yorkie Feedforward Loop

Indrayani Waghmare<sup>1,2</sup>, Karishma Gangwani<sup>1,3</sup> , Arushi Rai<sup>1</sup>, Amit Singh<sup>1,4,5</sup>  and Madhuri Kango-Singh<sup>1,4,5,\*</sup>

<sup>1</sup> Department of Biology, University of Dayton, Dayton, OH 45469, USA; indrayani\_waghmare@uclm.edu (I.W.); raia05@udayton.edu (A.R.); asingh1@udayton.edu (A.S.)

<sup>2</sup> Department of Biological Sciences, University of Massachusetts Lowell, Lowell, MA 01854, USA

<sup>3</sup> Computational Biology Department, St Jude Children’s Research Hospital, Memphis, TN 38105, USA

<sup>4</sup> Premedical Programs, University of Dayton, Dayton, OH 45469, USA

<sup>5</sup> Integrative Science and Engineering Centre (ISE), University of Dayton, Dayton, OH 45469, USA

\* Correspondence: mkangosingh1@udayton.edu; Tel.: +1-937-229-2531

**Simple Summary:** Cancer genomics and transcriptomics have revealed genes and pathways altered in several cancers. These studies have provided valuable information about cancer cells, their origin, oncogenic processes, and signaling pathways. An emerging challenge is to further characterize activity levels and interactions of pathways to develop a deeper understanding of how specific alterations in these interactions promote tumor growth. *Drosophila* with its sophisticated genetics has proved valuable in studying cooperative oncogenesis. Using *Drosophila* tumor models, we report a tumor cell-specific network comprising four pathways. We show that Wingless and effector caspase Dronc direct a signal amplification loop involving JNK and Hippo-effector Yorkie (Yki). Our studies provide evidence from in vivo studies regarding the organization of tumor-promoting oncogenic pathways, which may be useful in developing precise and effective approaches for pathway inhibition. These pathways are evolutionarily conserved from flies to humans, suggesting that findings from flies can be extrapolated to mammalian cancers.



**Citation:** Waghmare, I.; Gangwani, K.; Rai, A.; Singh, A.; Kango-Singh, M. A Tumor-Specific Molecular Network Promotes Tumor Growth in *Drosophila* by Enforcing a Jun N-Terminal Kinase–Yorkie Feedforward Loop. *Cancers* **2024**, *16*, 1768. <https://doi.org/10.3390/cancers16091768>

Academic Editor: Athanasios G. Papavassiliou

Received: 7 March 2024

Revised: 22 April 2024

Accepted: 25 April 2024

Published: 2 May 2024



**Copyright:** © 2024 by the authors. Licensee MDPI, Basel, Switzerland. This article is an open access article distributed under the terms and conditions of the Creative Commons Attribution (CC BY) license (<https://creativecommons.org/licenses/by/4.0/>).

**Abstract:** Cancer cells expand rapidly in response to altered intercellular and signaling interactions to achieve the hallmarks of cancer. Impaired cell polarity combined with activated oncogenes is known to promote several hallmarks of cancer, e.g., activating invasion by increased activity of Jun N-terminal kinase (JNK) and sustained proliferative signaling by increased activity of Hippo effector Yorkie (Yki). Thus, JNK, Yki, and their downstream transcription factors have emerged as synergistic drivers of tumor growth through pro-tumor signaling and intercellular interactions like cell competition. However, little is known about the signals that converge onto JNK and Yki in tumor cells and enable tumor cells to achieve the hallmarks of cancer. Here, using mosaic models of cooperative oncogenesis (*Ras<sup>V12</sup>,scrib<sup>-</sup>*) in *Drosophila*, we show that *Ras<sup>V12</sup>,scrib<sup>-</sup>* tumor cells grow through the activation of a previously unidentified network comprising Wingless (Wg), Dronc, JNK, and Yki. We show that *Ras<sup>V12</sup>,scrib<sup>-</sup>* cells show increased Wg, Dronc, JNK, and Yki signaling, and all these signals are required for the growth of *Ras<sup>V12</sup>,scrib<sup>-</sup>* tumors. We report that Wg and Dronc converge onto a JNK–Yki self-reinforcing positive feedback signal-amplification loop that promotes tumor growth. We found that the Wg–Dronc–Yki–JNK molecular network is specifically activated in polarity-impaired tumor cells and not in normal cells, in which apical-basal polarity remains intact. Our findings suggest that the identification of molecular networks may provide significant insights into the key biologically meaningful changes in signaling pathways and paradoxical signals that promote tumorigenesis.

**Keywords:** apical basal polarity; cancer; *Drosophila*; imaginal discs; Wingless; Hippo; JNK; caspase

## 1. Introduction

Over the past decade, genomic, transcriptomic, and proteomic data from several cancers have revealed the genetic alterations and changes in gene expression and epigenetic modifications linked to several cancers [1–4]. These approaches have revealed the extensive differences between normal and cancer cells, as well as the effects of cancer on multiple genes and signaling pathways [3]. Although these studies have provided valuable information about cancer cells, their origin, oncogenic processes, and signaling pathways, efforts now need to be directed at further characterizing tumors. For example, which proteins are expressed in the same cancer cell and are likely to physically interact? Which signaling pathways play decisive roles in promoting cell proliferation, survival, and metastasis in the different stages of cancer? Does the intricate distribution or clustering of ligand receptors affect cell–cell interactions [5]? For this, complementary approaches with *in vivo* models that allow manipulation of multiple genes (that represent the key cancer driver mutations) are required.

*Drosophila*, the common fruit fly, represents an efficient model organism to modulate the expression of multiple genes to study the signaling crosstalk that promotes tumor growth and progression [6,7]. Models of cooperative oncogenesis in *Drosophila*, such as clonal tumors induced by the activation of oncogenic Ras ( $Ras^{V12}$ ) in polarity-deficient *scribble* (*scrib*) [ $Ras^{V12}$  *scrib*<sup>−</sup>], *lethal giant larva* (*lgl*), or *discs large* (*dlg*) mutant cells, show classic hallmarks of aggressive cancer growth exemplified by increased proliferation rate, reduced apoptosis and differentiation, and metastasis [8–11]. These models have been instrumental in establishing the links between the deregulation of cell polarity and increased signaling from Jun N-terminal kinase (JNK) and Yorkie (Yki), effectors of two key signaling pathways that regulate cell proliferation and apoptosis [12–16]. However, the upstream mechanisms by which JNK and Yki activation promote aggressive metastatic growth during oncogenic cooperation remain poorly defined.

We investigated the changes in signaling interactions to decipher how oncogenic cooperation [ $Ras^{V12}$ , *scrib*<sup>−</sup>] promotes tumor growth. Herein, we show that the  $Ras^{V12}$ , *scrib*<sup>−</sup> tumors grow aggressively by upregulating a previously unidentified molecular network comprising the Wingless (*Wg*, the *Drosophila* homolog of mammalian Wnt1), the effector caspase *Dronc* (*Drosophila* homolog of mammalian Caspase 9), JNK, and Yki (*Drosophila* homolog of Hippo effectors YAP/TAZ in mammals). The upregulation of these signals promotes the growth of  $Ras^{V12}$ , *scrib*<sup>−</sup> tumors, and the depletion of these signals reverses these phenotypes. These signals are well-known for their roles in patterning and growth control [17–21] and intercellular interactions like cell competition [22–28]. We show that during oncogenic cooperation, these signals act together in a tumor cell-specific signaling network, in which *Wg* acts upstream of *Dronc* and regulates JNK and Yki. JNK activity changes from pro-apoptosis to pro-proliferation due to a paradoxical signaling switch that ultimately promotes Yki activity. We demonstrate that in  $Ras^{V12}$ , *scrib*<sup>−</sup> tumor cells, Yki, in turn, upregulates JNK activity, causing the robust activation of both JNK and Yki. This bidirectional regulatory interaction results in the formation of a self-reinforcing JNK-Yki positive feedback signal-amplification loop downstream of *Wg* and *Dronc*. We show that this molecular network is sufficient to induce tumorigenesis in other contexts of oncogenic cooperation (such as *en* > *Yki*, *scrib*<sup>−</sup>, or  $Ras^{V12}$ //*scrib*<sup>−</sup> [interclonal tumor model [10]]). Taken together, our data strongly support the functional significance of molecular networks rather than individual signals in cancer cells and provide novel insights into the molecular pathways and paradoxical signals that play a key role in tumor growth and progression.

## 2. Materials and Methods

### 2.1. Fly Stocks

The studies described here are conducted on *Drosophila melanogaster*, the common fruit fly. All flies were reared in a standard cornmeal–agar–molasses medium containing Tegosept and propionic acid. All fly stocks used in this study are described in Flybase (<http://flybase.bio.indiana.edu>) accessed on 1 March 2024.

The following stocks were used in this study: Canton-S, *FRT82B* (BL#5619), *FRT82B scrib<sup>7b3</sup>* (DGRC#111422), *FRT82B scrib<sup>2</sup>* [29], *FRT82B scrib<sup>2</sup> TubGAL-80* (this study), *diap1-lacZ* (BL#12093), *dronc<sup>1.7kb-lacZ</sup>* [30], *ex<sup>679</sup>-lacZ* [31], *wg-lacZ* [32], *AyGAL4*, *UAS-GFP* [33], *en-GAL4* (BL#1973), *UAS-GFP* (BL#1521), *FRT82B Ubi-GFP* (BL#5188), *FRT82B Tub-GAL80* (BL#5135), *MS1096-Gal4* (BL#8860), *UAS-P35* (BL#5072), *UAS-Ras<sup>V12</sup>* (BL#4847), *UAS-sgg<sup>S9A</sup>* (BL#5255), *UAS-Bsk<sup>DN</sup>* (BL#6409), *UAS-dronc<sup>RNAi</sup>* (gift from A. Bergmann, 8091R-1 from NIG-Fly (<http://www.shigen.nig.ac.jp/fly/nigfly/index.jsp>) accessed on 1 March 2024), *UAS-Yki<sup>N+CRNAi</sup>* [34], *UAS-proDronc* (gift from A. Bergmann), *UAS-jun<sup>aspv</sup>* [35], *UAS-Arm<sup>S10</sup>* (BL#4782), and *UAS-Yki* [36].

## 2.2. Generation of Somatic Clones

To make MARCM clones, we crossed *eyFLP* or *UbxFLP*; *AyGAL4 UASGFP*; *FRT82B Tub-GAL80* virgins with males of the appropriate genotypes. Heat shock-mediated “Flp-out” clones were generated by giving a 7 min heat shock at 37 °C to second instar larvae generated by crossing *AyGAL4 UASGFP* flies with *UAS Yki*. “Flp-out” clones were also generated by crossing *yw hsFLP*; *enGAL4 ex<sup>697</sup>-lacZ*; *FRT82B UbiGFP* flies with *UAS Yki*; *FRT82B scrib<sup>2</sup>* flies (for *en > Yki*; *scrib<sup>-</sup>* clones Figure 5). Interclonal oncogenic cooperation studies were performed by crossing *yw eyFLP*; *AyGAL4 UASGFP*; *FRT82B Tub-GAL80 scrib<sup>2</sup>* virgins with *yw hsFLP*; +; *UASRas<sup>V12</sup> FRT82B* males. All experiments were performed at 25 °C unless otherwise specified.

## 2.3. Immunohistochemistry and Image Acquisition

Immunohistochemistry was performed following our published protocol [37]. Briefly, imaginal discs from wandering 3rd instar larvae were dissected in 1XPBS (phosphate buffered saline), fixed in 4% paraformaldehyde (PFA) for 20 min (min) at room temperature (RT), washed 3 × 10 min each in 1XPBST (1XPBS + 0.2% Triton X-100), and blocked in PBSTN (PBST+ 2% Normal donkey serum) for 1 h before incubation with primary antibody at 4 °C overnight. The samples were then washed 3 × 10 min each in 1XPBST, incubated in an appropriate secondary antibody for two hours at RT, washed in 1XPBST for 20 min, and mounted in Vectashield (Vector Laboratories Inc., Burlingame, CA, USA).

The following primary antibodies were used: rabbit anti-cleaved Caspase 3 (1:250), rabbit anti-DCP1 (1:100), and rabbit anti-pJNK (1:250) from Cell-Signaling Technology, Danvers, MA, USA, mouse anti-Wingless (1:100), mouse or rabbit anti-beta-galactosidase (1:100), mouse anti-MMP1 (1:250), and rat anti-E-Cadherin (dCAD2, 1:100) from DSHB, Iowa, IA, USA, guinea pig anti-Dronc (1:400, from Dr. H. D. Ryoo), mouse anti-DIAP1 (1:250, from Dr. B. Hayes), and rabbit anti-Yorkie (1:400, from Dr. K. Irvine). The secondary antibodies were donkey Fab fragments conjugated to Cy3 or Cy5 against rabbit, mouse, rat, or guinea pig hosts (Jackson ImmunoResearch Labs, West Grove, PA, USA).

Image acquisition: We used an Olympus Fluoview 1000 confocal microscope to acquire projections of Z-stacks of confocal images. To enable comparison between samples, all images in an experimental group were acquired at identical magnification and similar imaging conditions. The final figures were made using Adobe Photoshop CS6.

## 2.4. Statistical Analyses

Statistical analyses were performed using Microsoft Excel 2013. The magnetic lasso tool was used for clone size comparison (Figures 1A and 2A Wild type n = 11, rest n = 25). Mean pixel values of clone area were obtained using the Histogram function in Photoshop CS6 and analyzed using the non-parametric Mann–Whitney test (two-tailed), assuming statistical significance at  $p < 0.05$ . Signal intensity levels for both inside (GFP-positive) and outside (GFP-negative), the clones were obtained using the histogram function in Adobe Photoshop CS6 (n = 5). The average wild-type values were used to find the normalization factor to determine and calculate differences in intensity levels between wild-type, *scrib<sup>-</sup>*, *Ras<sup>V12</sup>*, and *Ras<sup>V12</sup>; scrib<sup>-</sup>* clones for all antibodies tested. Bar scatterplots were then generated to show fold-change in Dronc, Wg, *dronc<sup>1.7kb-lacZ</sup>*, *wg-lacZ*, *diap1-lacZ*, pJNK

levels (Figures 1 and S1), and DIAP1 (Figures 2F and S3). Similarly, the normalization factor was calculated using wild-type values (GFP-negative areas) to assess changes in the expression of *Wg* (Figure 3), *Yki*, *pJNK*, and *Dronc* (Figure 4). Statistical significance ( $p < 0.05$ ) was tested using a non-parametric Mann–Whitney test (two-tailed), and all graphs were plotted using GraphPad Prism9.0.

### 2.5. qRT-PCR

RNA was extracted from eye imaginal discs from wandering third instar larvae. At least 40–50 discs were collected per genotype in TRIzol. The ZYMO RNA Clean and Concentrator Kit was used for RNA extraction. To prepare cDNA, 200 ng/ $\mu$ L RNA/sample was reverse transcribed using the cDNA synthesis kit (Cytiva, Danaher Corporation, Washington, DC, USA). qRT-PCRs were performed in triplicate per sample using the iQ SYBER Green Supermix (Bio-Rad Laboratories, Hercules, CA USA) on an iCycler iQ™ Real-Time PCR Detection System (Bio-Rad Laboratories, Hercules, CA USA). Three biological and three technical repeats were performed for each experiment, and data were analyzed using the ddCt method.

The following primers (IDT) were used:

*wg*: Forward primer: 5' CGT CAG GGA CGC AAG CAT A-3'

Reverse Primer: 5' ATT GTG CGG GTT CAG TTG G-3'

*dronc*: Forward primer: 5' CGA TGG ATC TGT GGT CGA TAT G-3'

Reverse Primer: 5' GGC TTC GCT CGT CTT CTT TA-3'

*Gapdh*: Forward primer: 5' TAA ATT CGA CTC GAC TCA CGG T-3'

Reverse Primer: 5' CTC CAC CAC ATA CTC GGC TC-3'

Statistical analyses were performed using the non-parametric Mann–Whitney test (two-tailed), assuming statistical significance at  $p \leq 0.05$ . Graphs were plotted using GraphPad Prism9.0.

## 3. Results

### 3.1. *Ras*<sup>V12</sup>, *scrib*<sup>−</sup> Cells Grow Robustly and Induce JNK, Yki, Dronc, and Wg

To investigate the changes in intercellular interactions that promote tumor growth, we made *ey-FLP*- and *Ubx-FLP*-induced MARCM clones [GFP positive] in the eye (Figure 1A–C) and wing discs (Figure 1D,E) respectively and monitored clone size to assess tumor growth (Figure 1A). Compared to wild-type (Figure 1A), *scrib*<sup>−</sup> clones grew poorly (Figure S1A) [38]. Given that *scrib*<sup>−</sup> clones are competed out due to cell competition-mediated apoptosis [12,38], we blocked apoptosis by overexpressing *UASp35* (Figure S1B), a pan-Caspase inhibitor [39]. The inhibition of apoptosis improved the growth of *scrib*<sup>−</sup> clones (*scrib*<sup>−</sup>, *p35*, Figures 1A and S1C); however, the discs remain monolayered, and clones did not form invasive tumors (Figure S1C,C' and YZ sections in Figure S1C''). In contrast, the coexpression of oncogenic Ras (*UASRas*<sup>V12</sup>) in *scrib*<sup>−</sup> cells (*Ras*<sup>V12</sup>, *scrib*<sup>−</sup>) resulted in robust aggressive and invasive tumors [8] that grew severalfold compared to wild-type, *scrib*<sup>−</sup>, or *scrib*<sup>−</sup>, *p35* clones (Figure 1A). These data suggest that a paradoxical switch changes the ability of *scrib*<sup>−</sup> cells, and inter-cellular interactions may play a critical role in these observed effects. Next, to understand the nature of the intercellular interactions that may underlie the differences in clone sizes, we tested cell death by using an antibody against activated Caspase 3 [Casp3\*]. In comparison to wild-type clones (Figure 1B,B'), *Ras*<sup>V12</sup>, *scrib*<sup>−</sup> clones show cell death both inside and outside the clone, and interestingly, the bulk of the observed cell death was induced in wild-type cells surrounding the clone (Figures 1C,C' and S1B–B''). Similarly in the wing discs, compared to wild-type (Figure 1D), *Ras*<sup>V12</sup>, *scrib*<sup>−</sup> clones grew into large invasive tumors (Figures 1E and S1D). Taken together, these data suggested that the *Ras*<sup>V12</sup>, *scrib*<sup>−</sup> clones grow robustly. Therefore, as a next step, we tested if JNK, Yki, Dronc, and Wg, markers that have previously been linked to cell survival and proliferation during cell competition [22–24,40] were also affected in the *Ras*<sup>V12</sup> *scrib*<sup>−</sup> tumors.

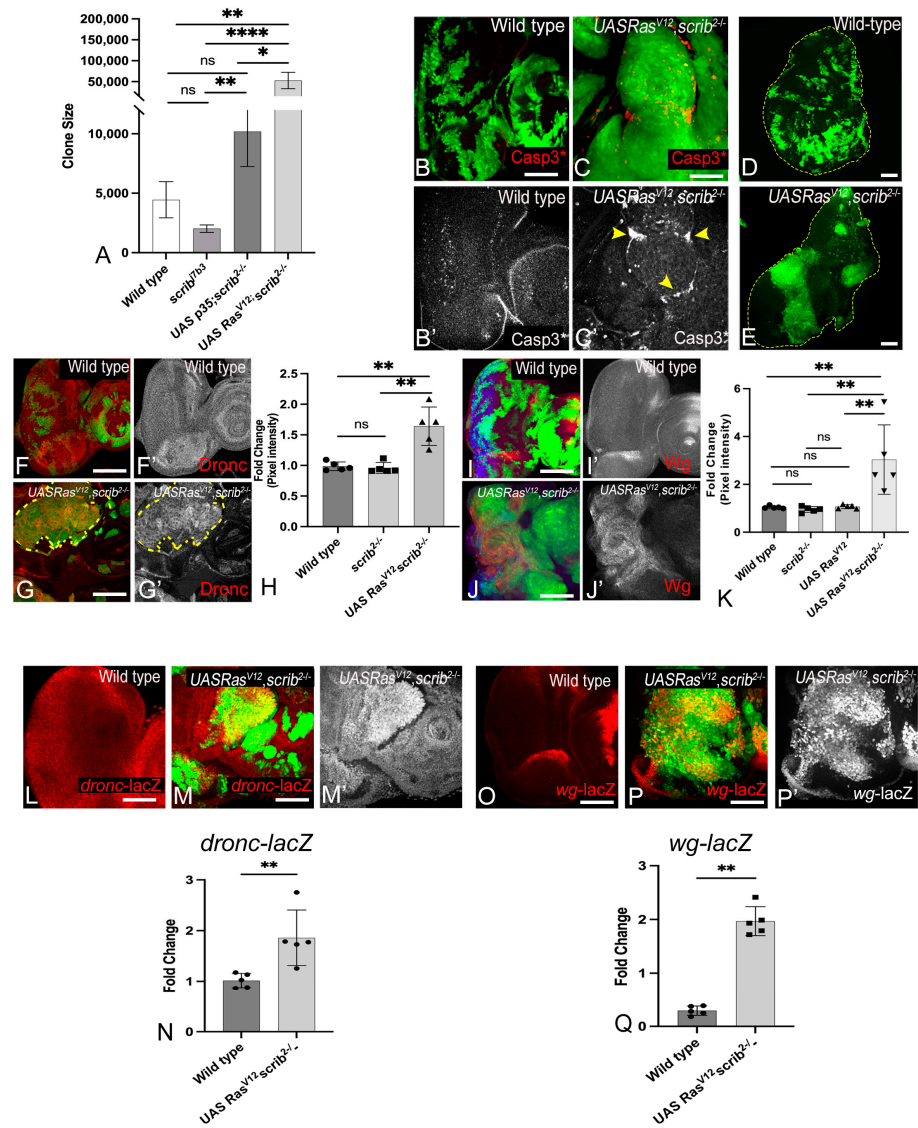


**Figure 1.** *Ras<sup>V12</sup> scrib<sup>-</sup>* cells grow robustly and induce Dronc and Wg. (A) Graph shows quantification of clone size comparing the growth of wildtype clones to *scrib<sup>-</sup>*, *p35; scrib<sup>-</sup>*, and *Ras<sup>V12</sup> scrib<sup>-</sup>* clones (n = 25). Panels show MARCM clones (GFP, green) from third-instar eye-antennal imaginal discs from (B) Wild-type, (C) *Ras<sup>V12</sup> scrib<sup>-</sup>*, and wing discs from (D) wild-type and (E) *Ras<sup>V12</sup> scrib<sup>-</sup>* respectively. Expression of cleaved caspase 3 [Casp3\*] antibody is shown in the eye discs (red in B,C, grey in B',C'). Yellow arrowheads mark dying cells in (C'). The outline of the wing disc is marked by a yellow dashed line in D,E. (F–H) Panels show Dronc expression (red, grey) in MARCM clones (green) induced in eye-antennal imaginal discs from (F,F') wild-type, and (G,G') *Ras<sup>V12</sup> scrib<sup>-</sup>*. (H) Bar scatter plot shows quantification of Dronc expression in MARCM clones in the indicated genotypes (n = 5). (I–K) Panels show expression and quantification of Wingless expression in eye discs from (I,I') wild-type and (J,J') *Ras<sup>V12</sup> scrib<sup>-</sup>* MARCM clones (green). (K) Bar scatter plot shows change in Wg expression in the indicated genotypes (n = 5). (L–N) *dronc<sup>1.7kb</sup>-lacZ* reporter expression (red, grey) in (L) wild-type and (M,M') *Ras<sup>V12</sup> scrib<sup>-</sup>* MARCM clones (green), quantified in (N). (O–Q) *wg-lacZ* reporter expression (red, grey) in (O) wild-type and (P,P') *Ras<sup>V12</sup> scrib<sup>-</sup>* MARCM clones (green), quantified in (Q). In all graphs, error bars show standard error of means (SEM). Statistical significance was calculated using Mann-Whitney test, where ns denotes *p*-value ≥ 0.05, and asterisks show significant interactions \* *p*-value ≤ 0.05, \*\* *p*-value ≤ 0.01, and \*\*\*\* *p*-value ≤ 0.0001. Disc orientation is identical in all panels. Scale bar = 25 μM.

JNK and Yki are known to interact in a context-dependent manner [12–14,41], and increased JNK or Yki activity has been linked to tumor growth [12,42–45]. In contrast, the

elimination of *scrib*<sup>-</sup> cells by cell competition involved JNK-dependent suppression of Yki activity [12,38,46–48]. To test Yki activity, we employed the Yki-reporter, *diap1-lacZ*, which is expressed ubiquitously in wild-type (Figure S1E) discs. Increased Yki activity due to Yki overexpression in “Flp-out” (*AyGAL4 > Yki*) clones showed the robust induction of *diap1-lacZ* (Figure S1F,F’). In the *Ras*<sup>V12</sup>,*scrib*<sup>-</sup> clones, *diap1-lacZ* was strongly induced (Figure S1G,G’). Interestingly, *diap1-lacZ* was also induced in peri-tumoral cells (non-cell autonomously in wild-type cells) abutting the *Ras*<sup>V12</sup>,*scrib*<sup>-</sup> tumors (Figure S1G’). The normalized pixel intensity from the controls and experimental groups was quantified and showed a significant increase in *Ras*<sup>V12</sup>,*scrib*<sup>-</sup> clones (Figure S1H). Compared to wild-type (Figure S1I,I’), pJNK was robustly induced in the *Ras*<sup>V12</sup>,*scrib*<sup>-</sup> clones (Figure S1J,J’, quantified in Figure S1K). Thus, consistent with previous data, JNK and Yki activities were simultaneously upregulated in the *Ras*<sup>V12</sup>,*scrib*<sup>-</sup> tumors. We then investigated the signals that converge onto Yki and JNK to promote the growth of *Ras*<sup>V12</sup>,*scrib*<sup>-</sup> tumors.

Previous studies have shown that Dronc (the initiator caspase that induces apoptosis through activation of caspase 3) and Wg (the secreted ligand of the Wingless/Wnt pathway that acts as a mitogen) play critical roles in intercellular interactions like cell competition and compensatory proliferation [27,49–51]. Yki also transcriptionally regulates *dronc* and *wg* [52,53]. We tested levels of active Dronc using an antibody against Dronc<sup>CA</sup>, the activated form of Dronc [51], and Wg in the *Ras*<sup>V12</sup>,*scrib*<sup>-</sup> clones (Figure 1). Dronc is expressed ubiquitously in wild-type imaginal discs (Figure 1F,F’, quantified in Figure 1H), and its levels remained unaffected in *scrib*<sup>-</sup> cells in the wild-type background (Figure 1H). Therefore, wild-type Dronc levels may be sufficient for the elimination of *scrib*<sup>-</sup> cells in the presence of elevated pJNK levels. In comparison, Dronc was strongly upregulated in *Ras*<sup>V12</sup>,*scrib*<sup>-</sup> cells (Figure 1G,G’). Quantification showed that Dronc levels were significantly upregulated (1.7-fold) in *Ras*<sup>V12</sup>,*scrib*<sup>-</sup> cells compared to either wild-type or *scrib*<sup>-</sup> cells (Figure 1H). Taken together, these data suggested that Dronc plays a non-apoptotic role and promotes *Ras*<sup>V12</sup>,*scrib*<sup>-</sup> tumor growth. In wild-type eye discs, Wg is expressed at the lateral margins anterior to the morphogenetic furrow (Figure 1I,I’, quantified in Figure 1K) [32]. This pattern of Wg expression was unaltered in *scrib*<sup>-</sup> cells generated in the wild-type background (Figure 1K). In *Ras*<sup>V12</sup>,*scrib*<sup>-</sup> clones, Wg was robustly induced (Figure 1J,J’). When compared to wild-type or *scrib*<sup>-</sup> cells, Wg expression was significantly upregulated (2.7-fold) in *Ras*<sup>V12</sup>,*scrib*<sup>-</sup> cells (Figure 1K), suggesting that the steep upregulation of Wg levels in *Ras*<sup>V12</sup>,*scrib*<sup>-</sup> may itself promote super-competition by promoting proliferation through its mitogenic functions.

Next, we checked if *dronc* and *wg* transcription was affected in *Ras*<sup>V12</sup>,*scrib*<sup>-</sup> cells using the *dronc*<sup>1.7kb</sup>-*lacZ* (Figure 1L–M’) and *wg-lacZ* (Figure 1O–P’) reporters, quantified in Figure 1N,Q, respectively. We found that compared to the wild-type (Figure 1L), *dronc*<sup>1.7kb</sup>-*lacZ* expression was robustly induced in the *Ras*<sup>V12</sup>,*scrib*<sup>-</sup> clones (Figure 1M,M’). Similarly, the normal pattern of *wg-lacZ* expression in eye discs (Figure 1O) was disrupted due to ectopic induction of *wg-lacZ* in *Ras*<sup>V12</sup>,*scrib*<sup>-</sup> clones (Figure 1O’). We confirmed the increased expression of *dronc* and *wg* in *Ras*<sup>V12</sup>,*scrib*<sup>-</sup> clones using qRT-PCR (Figure S2). The upregulation of *dronc* and *wg* in the tumor cells suggests that these genes promote tumor growth, possibly by co-opting compensatory mechanisms in which *dronc* plays a non-apoptotic role and *wg* plays a mitogenic role. Taken together, these data suggest that four signals associated with intercellular interactions (Yki, JNK, Wg, caspases) were upregulated in aggressively growing *Ras*<sup>V12</sup>,*scrib*<sup>-</sup> tumors.

### 3.2. *Ras*<sup>V12</sup>,*scrib*<sup>-</sup> Tumors Require JNK, Yki, Dronc, and Wg for Growth

To understand if some or all of these signals played a key role in the aggressive growth of *Ras*<sup>V12</sup>,*scrib*<sup>-</sup> tumors, we tested their requirement by independently down-regulating these signals in *Ras*<sup>V12</sup>,*scrib*<sup>-</sup> clones (Figure 2). To achieve this, we used well-established transgenes, for example, RNAi, to knockdown *Dronc*, which impairs caspase-mediated signaling [*UAS-Dronc*<sup>RNAi</sup>] [52], the dominant-negative form of Bsk, which is a potent suppressor of JNK signaling [*UAS-Bsk*<sup>DN</sup>] [38], *UAS-Sgg*<sup>S9A</sup>, which dominantly blocks Wg signaling [54], and *UAS-Yki*<sup>N+CRNAi</sup>, which causes the inactivation of Yki-mediated signaling [34].

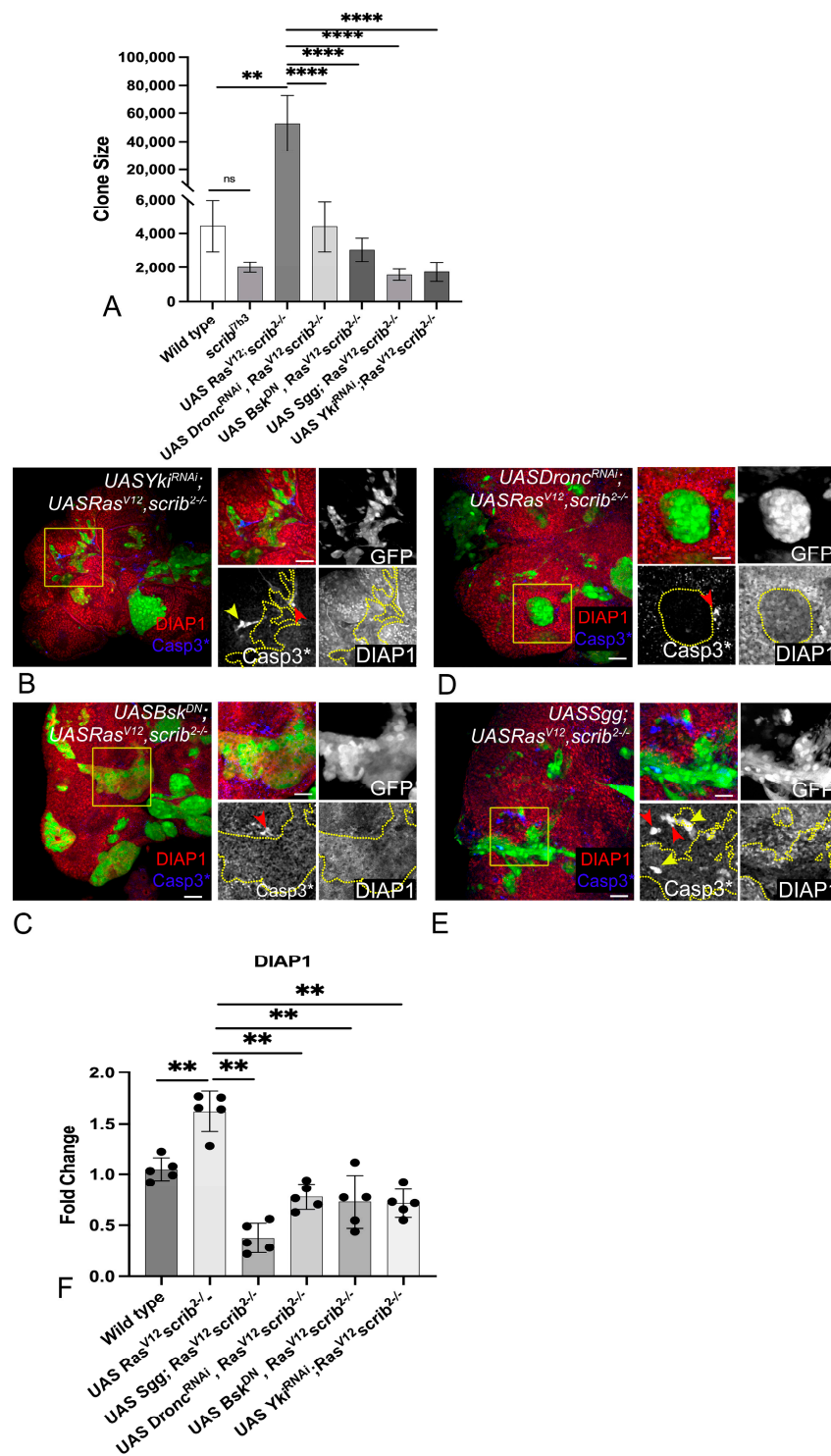


**Figure 2.** *Ras<sup>V12</sup> scrib<sup>-</sup>* tumors require Dronc, Wg, JNK, and Yki for growth. **(A)** Bar graph shows quantification of clone size of the following genotypes: wild-type, *scrib<sup>-</sup>*, *Ras<sup>V12</sup> scrib<sup>-</sup>*, *UASDronc<sup>RNAi</sup> UASRas<sup>V12</sup> scrib<sup>-</sup>*, *UASBsk<sup>DN</sup> UASRas<sup>V12</sup> scrib<sup>-</sup>*, *UASSgg<sup>S9A</sup> UASRas<sup>V12</sup> scrib<sup>-</sup>*, and *UASYki<sup>N+CRNAi</sup> UASRas<sup>V12</sup> scrib<sup>-</sup>* (n = 25) **(B–E)** Panels show DIAP1 (red) and Casp3\* (blue) expression in eye imaginal discs containing MARCM clones (green) of the following genotype: **(B)** *UASYki<sup>N+CRNAi</sup> UASRas<sup>V12</sup> scrib<sup>-</sup>*, **(C)** *UASBsk<sup>DN</sup> UASRas<sup>V12</sup> scrib<sup>-</sup>*, **(D)** *UASDronc<sup>RNAi</sup> UASRas<sup>V12</sup> scrib<sup>-</sup>*, and **(E)** *UASSgg<sup>S9A</sup> UASRas<sup>V12</sup> scrib<sup>-</sup>*. Clone areas highlighted by yellow boxes are further magnified in the image to the right, and split channel images in greyscale are presented for each genotype. Clone outlines are marked by the yellow dotted line, red arrowheads highlight

Casp3\* positive apoptotic cells outside the clones, whereas yellow arrowheads mark Casp3\* positive apoptotic cells inside the clones. (F) Bar scatter plot presents the fold change in DIAP1 levels comparing wild-type and *UASRas<sup>V12</sup> scrib<sup>-</sup>* to all tested genotypes (n = 5). In all graphs, error bars show standard error of means (SEM). Statistical significance was calculated using Mann-Whitney test, where ns denotes *p*-value  $\geq 0.05$ , and asterisks show significant interactions \*\* *p*-value  $\leq 0.01$ , and \*\*\*\* *p*-value  $\leq 0.0001$ . Disc orientation is identical in all panels. Scale bar = 25  $\mu\text{m}$ .

A comparison of clone sizes revealed that individual downregulation of the four signaling pathways significantly decreased the growth of the *Ras<sup>V12</sup>,scrib<sup>-</sup>* cells (Figure 2A–E). These findings suggested that the four signals are independently required for the aggressive growth of *Ras<sup>V12</sup>,scrib<sup>-</sup>* tumors. Therefore, we next tested if loss of cellular fitness or interactions amongst these signals was an underlying cause for the change in tumor size.

### 3.3. Downregulation of JNK, Yki, Dronc, and Wg Impairs Cellular Fitness

We hypothesized that the reduction in clone size was due to altered fitness within *Ras<sup>V12</sup>,scrib<sup>-</sup>* cells. First, we tested changes in DIAP1 levels (Figure 2B–E red, grey) in conditions where at least one of these four signals was downregulated (Figure 2B–F). As DIAP1 inhibits caspase activation, it protects cells from caspase-mediated apoptosis [55]. DIAP1 was ubiquitously expressed in wild-type cells (Figure S3A), downregulated in *scrib<sup>-</sup>* cells (Figure S3B, yellow arrowheads), and robustly induced in *Ras<sup>V12</sup>,scrib<sup>-</sup>* clones (Figure S3C). However, when Yki (Figure 2B), JNK (Figure 2C), Dronc (Figure 2D), or Wg (Figure 2E) were downregulated in *Ras<sup>V12</sup>,scrib<sup>-</sup>* clones (Figure 2C–E, yellow outline in grey channels), DIAP1 was downregulated (quantified in Figure 2F). This finding suggests that *Ras<sup>V12</sup>,scrib<sup>-</sup>* tumor cells had decreased survival and were susceptible to elimination by apoptosis (Figure 2B–E, blue, grey), when the tumor-promoting signals were downregulated. The downregulation of Yki (Figure 2B) or Wg (Figure 2E) resulted in apoptosis both inside (Figure 2B,E yellow arrowheads) and outside (Figure 2B,E, red arrowhead) the *Ras<sup>V12</sup>,scrib<sup>-</sup>* clones, suggesting that Wg and Yki protect *Ras<sup>V12</sup>,scrib<sup>-</sup>* tumors during competitive interactions. The downregulation of the JNK pathway (Figure 2C) or Dronc (Figure 2D) resulted in apoptosis at the clone boundary (Figure 2C,D, red arrowhead), but not within the clones, likely because these cell death regulators (JNK and Dronc) were suppressed in the clones. Taken together, these data suggested that the downregulation of the tumor-promoting signals impaired cellular fitness in *Ras<sup>V12</sup>,scrib<sup>-</sup>* cells.

These observations were further supported in control experiments, where we made MARCM clones in which we depleted each component of the molecular network in otherwise wild-type cells (Figure S4). Wg is a target of its own signaling [56–58]. Therefore, we made *UAS-Sgg<sup>S9A</sup>* control clones (Figure S3A,B) and confirmed that the endogenous expression of Wg was suppressed in *UAS-Sgg<sup>S9A</sup>* clones using anti-Wg antibody (shown by the yellow arrow in Figure S4B''). The downregulation of Wg signaling (Figure S4B red, Figure S4B'' grey) caused cell death (Figure S4A blue, Figure S4A''' grey) and the downregulation of DIAP1 (Figure S4A red, Figure S4A'' grey). However, the levels of pJNK (Figure S4B blue, Figure S4B''' grey) remained unaltered. The depletion of Dronc blocked cell death (Figure S4C blue, Figure S4C''' grey) and did not significantly affect DIAP1 (Figure S4C red, Figure S4C'' grey), Wg (Figure S4D red, Figure S4D'' grey), or pJNK (Figure S4D blue, Figure S4D''' grey) expression. Blocking JNK signaling (Figure S4E,F) showed similar effects to those of the downregulation of Dronc on DIAP1 (Figure S4E red, Figure S4E'' grey), cell death (Figure S4E blue, Figure S4E''' grey), Wg (Figure S4F red, Figure S4F'' grey), or pJNK (Figure S4F blue, Figure S4F''' grey). The depletion of Yki (Figure S4G,H) resulted in the downregulation of DIAP1 (Figure S4G red, Figure S4G'' grey) and a strong non-cell autonomous induction of cell death (Figure S4G blue, Figure S4G''' grey). No significant effects on Wg (Figure S4H red, Figure S4H'' grey) or pJNK (Figure S4H blue, Figure S4H''' grey) were seen. Thus, Wg and Yki emerged as key signaling proteins among these four pathways.

### 3.4. Wg, Dronc, JNK, and Yki Form a Molecular Network in *Ras<sup>V12</sup>,scrib<sup>-</sup>* Tumors

Next, we tested if Wg, Dronc, JNK, and Yki regulated one another to promote the aggressive growth of *Ras<sup>V12</sup>,scrib<sup>-</sup>* tumors (Figure 3). The downregulation of Wg signaling in *Ras<sup>V12</sup>,scrib<sup>-</sup>* cells (Figure 3A) resulted in small tumors and a reduction in Wg expression (Figure 3A red, A'' grey). Interestingly, depleting Dronc (Figure 3B), JNK (Figure 3C), or Yki (Figure 3D) caused a significant decrease in clone size, but Wg was strongly induced in these clones (Figure 3B''–D''). It is notable that Wg is induced in both a cell-autonomous and non-cell-autonomous manner. Normalized signal intensity is quantified in Figure 3E. Thus, we identified that Wg acts upstream of Dronc, JNK, and Yki in the network of signals that promote *Ras<sup>V12</sup>,scrib<sup>-</sup>* tumor growth.

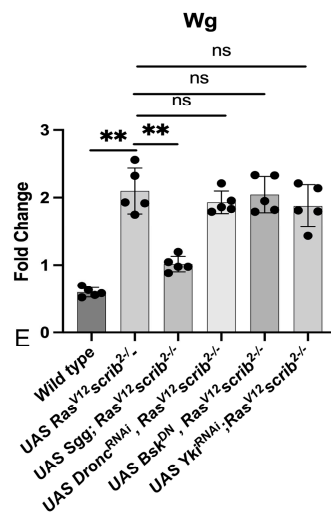
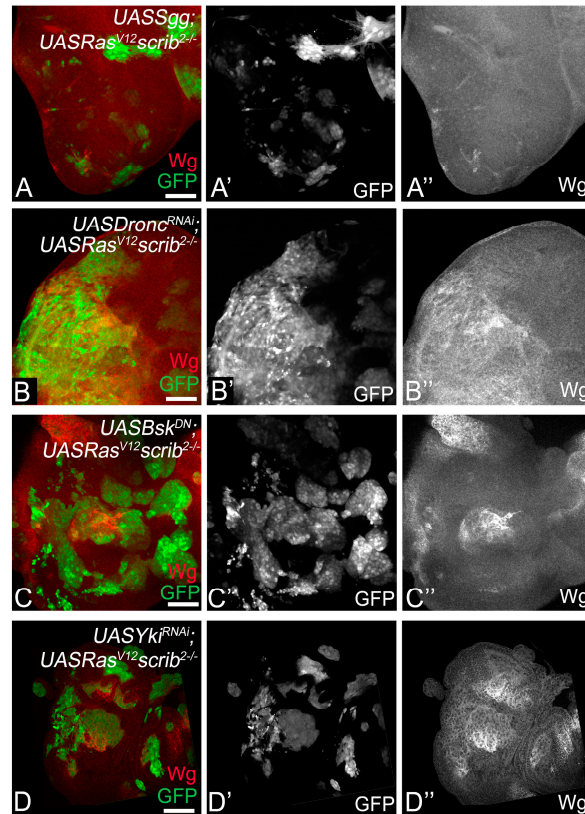


**Figure 3.** Wg acts upstream of the molecular network. Panels show Wg expression (red in A–D, grey in A''–D'') in MARCM clones (green in A–D, grey in A'–D') of the following genotype:

(A)  $UASSgg^{S9A} UASRas^{V12} scrib^{-}$ , (B)  $UASDronc^{RNAi} UASRas^{V12} scrib^{-}$ , (C)  $UASBsk^{DN} UASRas^{V12} scrib^{-}$ , and (D)  $UASYki^{N+CRNAi} UASRas^{V12} scrib^{-}$ . (E) Bar scatter plot presents the fold change in Wg levels comparing wild-type and  $UASRas^{V12} scrib^{-}$  to all tested genotypes ( $n = 5$ ). Error bars show standard error of means (SEM). Statistical significance was calculated using Mann-Whitney test, where ns denotes  $p$ -value  $\geq 0.05$ , and asterisks show significant interactions  $** p$ -value  $\leq 0.01$ . The magnification and orientation of discs are identical in all panels. Scale bar = 25  $\mu$ m.

To test if these signals interact with each other, we checked the effects of Yki depletion ( $Yki^{RNAi}; Ras^{V12}, scrib^{-}$ , Figure 4A–D) on Dronc (Figure 4A) and pJNK expression (Figure 4B). The depletion of Yki (confirmed in Figure 4C red, C' grey) did not affect the induction of Dronc (Figure 4A blue, A' grey); however, pJNK expression was downregulated in these clones (Figure 4B red, B' grey). We quantified the normalized mean grey values and plotted the fold change comparing wild-type to  $Ras^{V12}, scrib^{-}$  and  $Yki^{RNAi}; Ras^{V12}, scrib^{-}$ . Graphs show the significant downregulation of Yki and pJNK, whereas Dronc accumulation was not affected (Figure 4D). Next, we downregulated JNK signaling (Figure 4E–G) through the overexpression of a dominant negative form of basket (Bsk) in  $Ras^{V12}, scrib^{-}$  ( $Bsk^{DN}; Ras^{V12}, scrib^{-}$ ), which results in the downregulation of pJNK (Figure 4E blue, E' grey), but Dronc expression remained upregulated in these clones (Figure 4E red, E' grey). Interestingly, Yki expression was also depleted in  $Bsk^{DN}; Ras^{V12}, scrib^{-}$  cells (Figure 4F red, F' grey). We plotted the normalized fold change in the expression of Dronc, Yki, and pJNK, which confirms these effects (Figure 4G). Interestingly, the downregulation of Dronc ( $Dronc^{RNAi}; Ras^{V12}, scrib^{-}$ , Figure 4H–J) in  $Ras^{V12}, scrib^{-}$  cells (Figure 4H red, H' grey) showed the downregulation of JNK (Figure 4H blue, H'' grey) and Yki (Figure 4I red, I' grey). Quantification shows that compared to wild-type or  $Ras^{V12}, scrib^{-}$ , the significant downregulation of Yki and JNK is seen in  $Dronc^{RNAi}; Ras^{V12}, scrib^{-}$  clones (Figure 4J). The downregulation of Wg (Figure 4K–M) in  $Ras^{V12}, scrib^{-}$  cells ( $Sgg^{S9A}; Ras^{V12}, scrib^{-}$ ) showed the downregulation of Dronc (Figure 4K red, K' grey), pJNK (Figure 4K blue, K'' grey), and Yki (Figure 4L red, L' grey). Quantification of the effects of downregulation of Wg revealed significant downregulation of Dronc, Yki, and pJNK compared to  $Ras^{V12}, scrib^{-}$  clones (Figure 4M). These data show that Dronc levels remain upregulated and comparable to  $Ras^{V12}, scrib^{-}$  cells in combinations in which either Yki (Figure 4D) or JNK (Figure 4G) are downregulated. Thus, these data suggest that Dronc acts upstream of Yki and JNK in this signaling network. Furthermore, JNK and Yki regulate each other, suggesting that they may act in a feedforward loop downstream of Dronc. Overall, our data suggest that the growth of the  $Ras^{V12}, scrib^{-}$  clones depended on a network involving Wg-dependent activation of Dronc, which controls a JNK-Yki mediated signal amplification loop that sustains high levels of JNK and Yki activities.

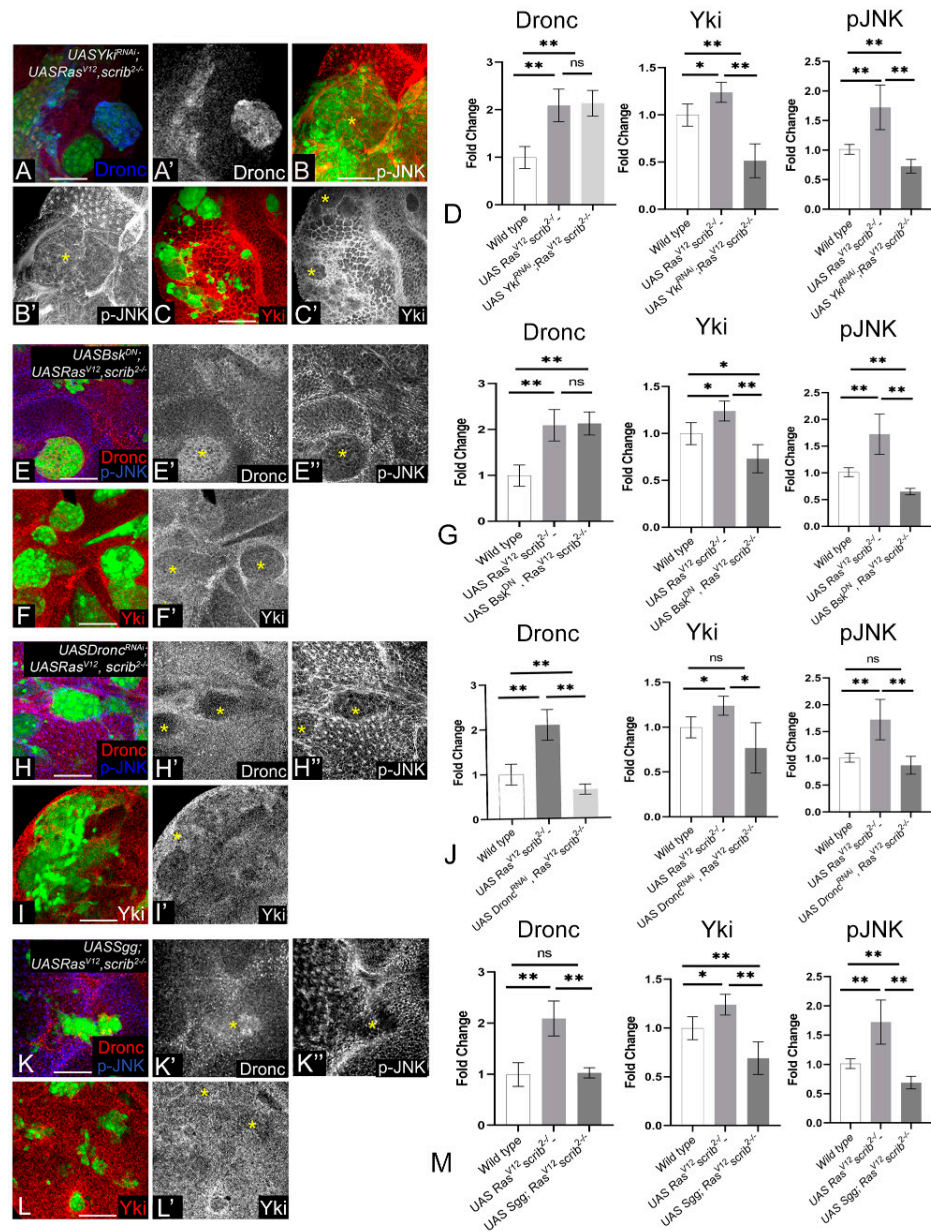


**Figure 4.** Wg, Dronc, JNK, and Yki form a molecular network in *Ras<sup>V12</sup> scrib<sup>-</sup>* clones. Panels show Dronc, Yki, and p-JNK expression in MARCM clones (green) when the molecular network is perturbed. (A–D) Panels show *UASYki<sup>RNAi</sup> UASRas<sup>V12</sup> scrib<sup>-</sup>* clones stained for Dronc ((A) blue, (A′) grey), pJNK ((B) red, (B′) grey) and Yki ((C) red, (C′) grey), quantified in (D). (E–G) *UASBsk<sup>DN</sup> UASRas<sup>V12</sup> scrib<sup>-</sup>* clones showing expression of Dronc ((E) red, (E′) grey), pJNK ((E) blue, (E′) grey), and Yki ((F) red, (F′) grey), quantified in (G). (H–J) Confocal images of *UASDronc<sup>RNAi</sup> UASRas<sup>V12</sup> scrib<sup>-</sup>* clones showing expression of Dronc ((H) red, (H′) grey), pJNK ((H) blue, (H′) grey), and Yki ((I) red, (I′) grey) are presented. The quantification of fold change is shown in (J). (K–M) Panels show confocal scans of *UASSgg<sup>S9A</sup> UASRas<sup>V12</sup> scrib<sup>-</sup>* clones stained for Dronc ((K) red, (K′) grey), pJNK ((K) blue, (K′) grey), and Yki ((L) red, (L′) grey), quantified in (M). The yellow asterisks mark representative MARCM clones in the grey channels. The quantifications in (D,G,J,M) show fold change comparison of normalized signal intensity between indicated genotypes, and error bars show SEM (standard error of means). Statistical significance was calculated using Mann-Whitney test, where ns denotes *p*-value  $\geq 0.05$ , and asterisks show significant interactions \* *p*-value  $\leq 0.05$ , \*\* *p*-value  $\leq 0.01$ . Disc orientation is identical in all panels. Scale bar = 25  $\mu$ m.

### 3.5. Cooperative Interactions Stimulate the Molecular Network and Tumor Growth

The preceding data led us to ask if oncogene activation, loss of polarity (*scrib*<sup>−</sup>), or cooperative interactions were important in stimulating the molecular network and tumor growth. The loss of polarity (*scrib*) alone is insufficient to induce aggressive growth in somatic clones (Figures 1 and S1) [8,9,12,38]; therefore, we tested the importance of cooperative interactions on the induction of the Wg–Dronc–JNK–Yki network and tumor growth. We tested two scenarios in which the loss of polarity could synergize with oncogene activation.

In the first scenario, we generated *scrib*<sup>−</sup> clones [GFP-negative clones in the *FRT82B Ubi-GFP* background generated by *hs-FLP*] in wing discs in which Yki was overexpressed [*UAS-Yki*] in the posterior compartment using *en-GAL4* [*en > Yki; scrib*<sup>−</sup>] (Figure 5). In the eye or wing discs, *scrib* mutant clones are susceptible to elimination by cell competition due to the upregulation of JNK (Figure S5A–B'), downregulation of Yki activity, as seen through the suppression of *diap1-lacZ* (Figure S5C–D' yellow arrowheads), and little to no effect on Dronc (Figure S5E) or Wg (Figure S5F) expression. Whereas, consistent with published data, the over-expression of Yki results in robust overgrowth due to the induction of Yki activity, leading to the upregulation of JNK [14,16], activation of DIAP1 (Figure S1F), ectopic induction of Wg [16], and suppression of Dronc [52]. Thus, the loss of *scrib* had clear and distinguishable effects from Yki overexpression (Figures 5 and S5) on all four signals. These distinct effects allowed an ideal opportunity to test altered signaling caused during oncogenic cooperation by Yki overexpression in *scrib* mutant cells. We found that *scrib*<sup>−</sup> clones grew to significantly larger sizes in the posterior (P) compartment in which Yki was overexpressed (Figure 5A–E) and showed reduced E-cadherin expression (Figure 5A, red, grey, red asterisk). Increased Yki activity in the posterior compartment was monitored by *ex-lacZ* expression (Figure 5B red, B' grey), which also allows marking the anterior–posterior (A/P) boundary (shown in the yellow dotted line in Figure 5). In addition to the increased *ex-lacZ* staining observed in the posterior compartment due to *yki* overexpression, *Yki* activity in the *scrib*<sup>−</sup> cells in the posterior compartment was very strongly induced within and around the clones (Figure 5B, outlined by the yellow line). We called this dramatic increase in Yki activity “super-induction”. In these clones, pJNK (Figure 5C red, C' grey), Wg (Figure 5D red, D' grey), and MMP1 (Figure 5E red, E' grey) were induced in and around the *scrib*<sup>−</sup> clones, potentially leading to the establishment of the JNK–Yki loop and invasiveness by the induction of MMP1. The Yki, pJNK, and Wg signals spread to several cells outside the *scrib*<sup>−</sup> clones, with Yki activity propagating the farthest (Figure 5B,B'). In contrast, the anterior (A) compartment *scrib*<sup>−</sup> clones (Figure 5B–E blue outline) behaved like clones in the wild-type background (Figure S1A) and were eliminated through cell competition. A comparison of the P and A compartment-specific clones suggested that the JNK–Yki signal amplification loop was activated specifically in the tumor cells in the P compartment in which cooperative interactions occurred due to Yki expression in *scrib*<sup>−</sup> cells.

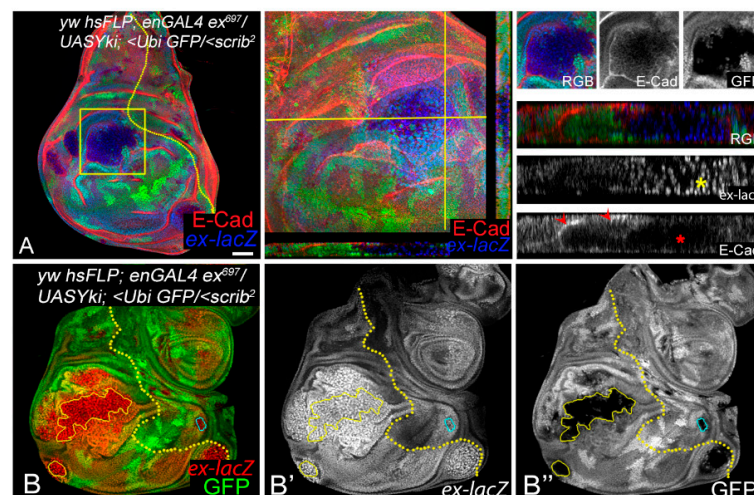
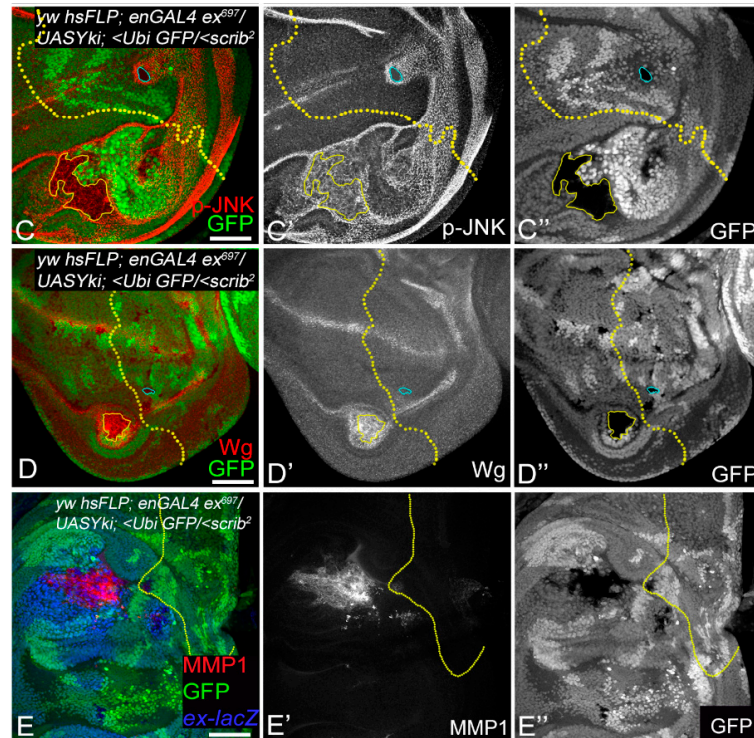
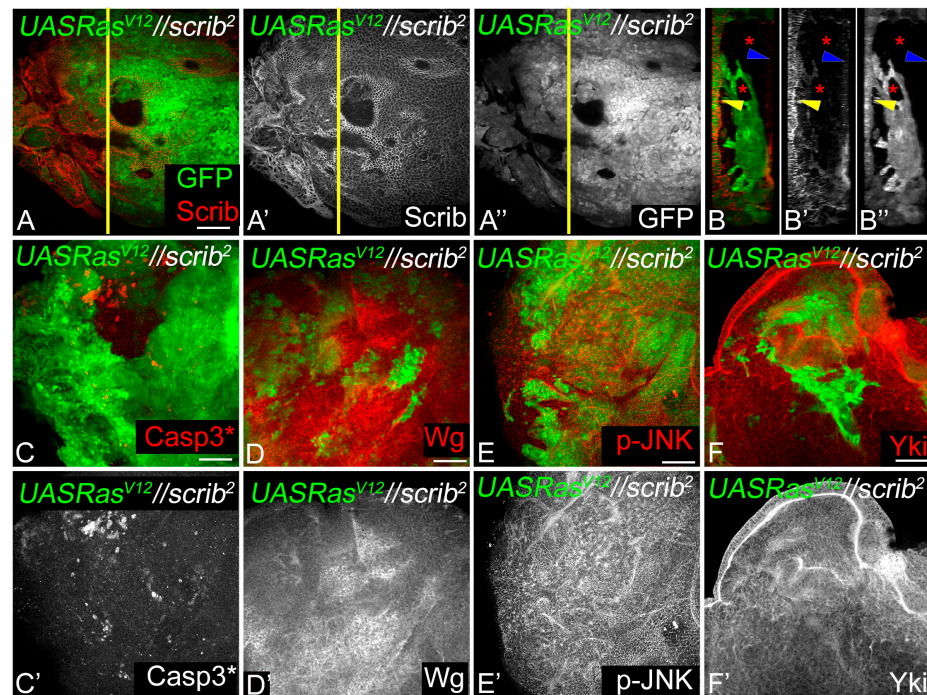


Figure 5. Cont.



**Figure 5.** Cooperative interactions induce the Wg–Dronc–JNK–Yki network to stimulate tumor growth. (A) Wing imaginal discs showing *en* > *Yki*, *scrib*<sup>−</sup> clones (GFP-negative) stained for *ex-lacZ* (using antibodies to β-gal, (A) blue) and E-cadherin (anti-dCAD2 antibodies, (A) red). The area highlighted by the yellow box is shown at higher magnification in the panels to the right. A cropped image of the clone is shown next to depict changes in polarity and growth. Yellow asterisks show the multi-layered appearance of nuclei positive for *ex-lacZ* within the *en* > *Yki*, *scrib*<sup>−</sup> clones, and red asterisks point toward the loss of E-cadherin in the XZ section (along the plain marked in the middle panel), and normal E-cadherin localization is highlighted by red arrows for comparison. (B) *Yki* activity as assessed by β-gal expression ((B) red, (B') grey) in *en* > *Yki*, *scrib*<sup>−</sup> clones is shown. (C–E) Wing discs containing *en* > *Yki*, *scrib*<sup>−</sup> clones (GFP negative) were assayed for ((C) red, (C') grey), ((D) red, (D') grey) or MMP1 ((E) red, (E') grey) expression. The *scrib*<sup>−/−</sup> clones in posterior compartment (solid yellow line) and anterior compartment (blue lines) are highlighted for each marker. In all images, the anterior–posterior compartment boundary is marked by a yellow dotted line drawn based on *ex-lacZ* expression. Images in (A,B) are at 20× magnification, and (C–E) are at 40× magnification. Posterior is to the left and dorsal is up in all discs. Scale bar = 25 μm.

In the second scenario, we tested if the Wg–Dronc–JNK–Yki network was activated during interclonal cooperation when *Ras*<sup>V12</sup> and *scrib*<sup>−</sup> cells were adjacent to each other (*Ras*<sup>V12</sup>//*scrib*<sup>−</sup>) [10]. Consistent with previous data, aggressive *Ras*<sup>V12</sup> tumors (GFP-positive) were formed adjacent to smaller *scrib*<sup>−</sup> clones (GFP negative, Figure 6A) [10]. Interestingly, the *Ras*<sup>V12</sup> clones extruded apically and showed a multi-layered invasive phenotype (Figure 6A–A'', Y–Z sections in Figure 6B–B''). The *Ras*<sup>V12</sup> clones showed robust growth despite the induction of cell death at the clone boundary between *Ras*<sup>V12</sup> (GFP-positive) and *scrib*<sup>−</sup> (GFP-negative) (Figure 6C,C') clones. The expression of Wg was robustly induced in the *scrib*<sup>−</sup> clones (Figure 6D,D'), whereas pJNK levels appear upregulated in both *scrib*<sup>−</sup> and *Ras*<sup>V12</sup> clones (Figure 6E,E') [10,38]. *Yki* expression showed higher nucleocytoplasmic distribution in the *Ras*<sup>V12</sup> clones (Figure 6F,F'). Taken together, these data suggest that the robust growth of the *Ras*<sup>V12</sup> clones was dependent on the interclonal signaling interactions with *scrib*<sup>−</sup> clones and involved caspases, *Yki*, Wg, and JNK signaling. Overall, these two experimental approaches reaffirmed that the induction of the molecular network was intimately linked to tumor growth in diverse scenarios.



**Figure 6.** Wg-Dronc-JNK-Yki network drives tumor growth during interclonal interactions. (A)  $Ras^{V12}/scrib^{-}$  interactions in eye discs show small  $scrib^{-}$  clones identified by loss of Scrib expression (red in A, grey in A') and adjacent  $Ras^{V12}$  clones (GFP positive green in A, grey in A'). (B–B'') The YZ projection of the yellow line in A shows a multi-layered  $Ras^{V12}$  clone (GFP). The red asterisks mark the  $scrib^{-}$  clones (GFP negative in B, B''), the yellow arrowhead marks the disc proper, and the blue arrowhead marks the peripodial membrane. (C–F) Eye discs show expression of Casp3\* (C red, C' grey), Wg (D red, D' grey), p-JNK (E red, E' grey), and Yki (F red, F' grey), in  $Ras^{V12}/scrib^{-}$  interclonal interactions. Note upregulation of Casp3\*, Wg and Yki at the boundary of  $Ras^{V12}$  clones. Scale bar = 25  $\mu$ m.

### 3.6. The Role of Apical–Basal Polarity in the Establishment of Tumor-Specific Molecular Networks

The Wg–Dronc–Yki–JNK network requirement in promoting tumor growth under various cooperative contexts raised the question if these four signals were sufficient to induce tumors in normal cells or if the loss of polarity is essential to form aggressive tumors. To test this, we first tested the effect of overexpressing Wg–Dronc–Yki–JNK in normal cells using the Gal4-UAS system in wing-imaginal discs. We used the wing hinge and pouch-specific *MS1096-Gal4* (Figure 7A) to drive the expression of transgenes overexpressing Yki (*UAS-Yki*), Dronc (*UAS-proDronc*), JNK (*UAS-jun<sup>aspv</sup>*), and Wg (*UAS-Arm<sup>S10</sup>*) [*MS1096 > Yki, pro-Dronc, jun<sup>aspv</sup>, Arm<sup>S10</sup>*], which would result in the activation of all four signals (Figure 7). In wild-type wing discs, DIAP1 (Figure 7B) and pJNK (Figure 7E) are ubiquitously expressed, whereas Wg is expressed in the wing hinge, wing margin, and notum (Figure 7D). Wild-type discs show few randomly dying cells marked by DCP-1 (Figure 7C). Interestingly, the coexpression of these transgenes resulted in hyperplasia of the wing pouch and hinge region (Figure 7E,G). We observed moderate upregulation of DIAP1 in the wing pouch region (Figure 7F') and increased cell death in the wing hinge region (Figure 7F''). Both Wg (Figure 7G,G') and pJNK are induced in a patchy pattern in the dorsal hinge region (Figure 7G,G''). In control experiments, the overexpression of individual transgenes revealed that the overexpression of Yki (*MS1096 > Yki*) is capable of driving hyperplasia and the upregulation of DIAP1, Wg, and pJNK (Figure S6A–B''). The overexpression of pro-Dronc (*MS1096 > proDronc*) did not affect disc growth very strongly and showed moderate upregulation of DIAP1, cell death, Wg, and pJNK (Figure S6C–D''), suggesting that pro-Dronc plays a role in promoting survival, but not cell proliferation. Overexpression of *jun<sup>aspv</sup>* (*MS1096 > jun<sup>aspv</sup>*) showed the most interesting effects by re-

ducing the size of the wing pouch due to strong suppression of DIAP1 and the induction of cell death (Figure S6E–E’). Although Wg and pJNK are induced in this combination (Figure S6F–F’), the excessive cell death in the wing pouch does not support the growth of these discs. The activation of the Wg pathway through the overexpression of Arm<sup>S10</sup> (*MS1096 > Arm<sup>S10</sup>*) resulted in the upregulation of DIAP1, Wg, and pJNK (Figure S6G–H’). In addition, mild to moderate levels of cell death were observed in the wing pouch (Figure S6G’). Taken together, these data suggest that although the coactivation of these transgenes results in increased growth or mild hyperplasia, the presence of normal wild-type cells with intact polarity does not allow for the establishment of the network that would drive the tumor growth.

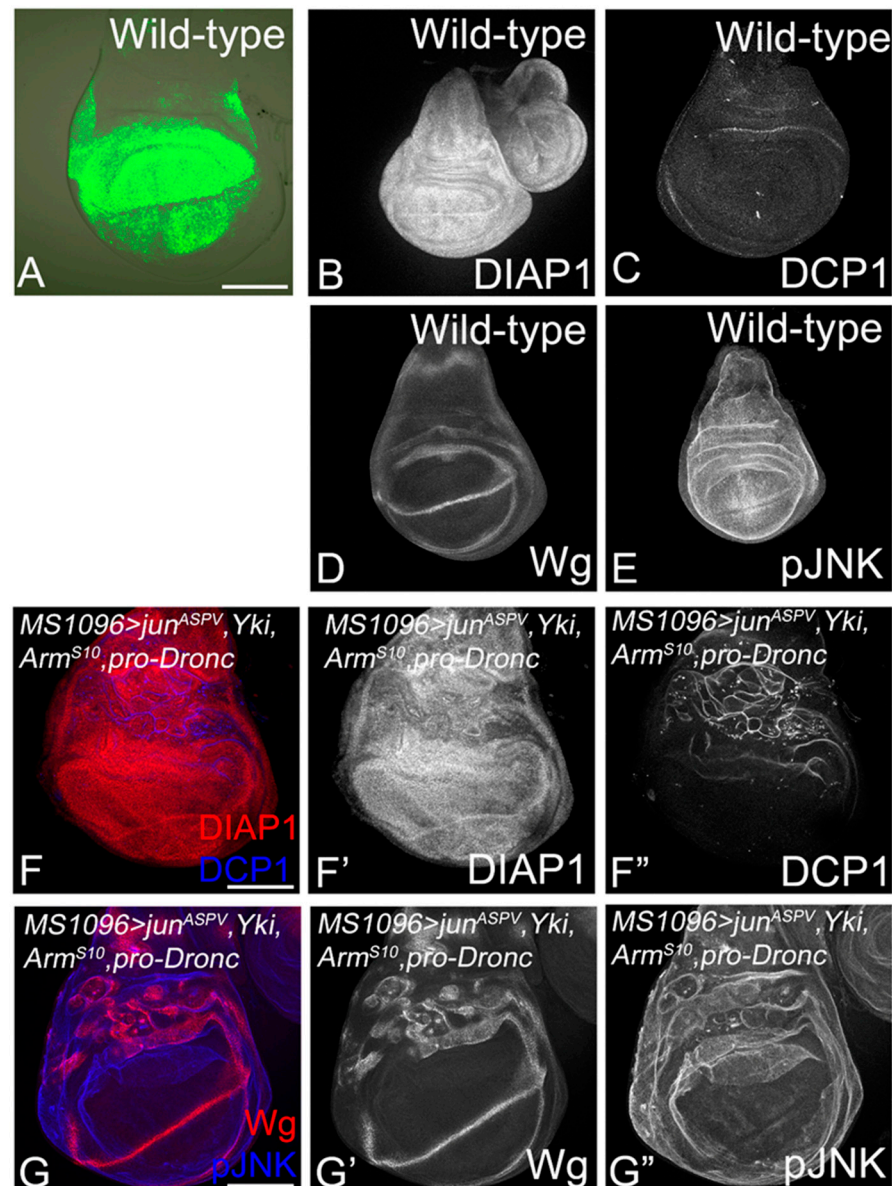


**Figure 7.** Loss of polarity is required for the Wg–Dronc–JNK–Yki network to drive tumor growth. (A–E) Control wing imaginal discs from (A) *MS1096 Gal4 > UASGFP*, and wild-type wing discs stained for (B) DIAP1, (C) DCP1, (D) Wg, and (E) pJNK are shown. (F–G’’) Panels show wing imaginal discs from *MS1096 Gal4 > UASjun<sup>ASPV</sup>, UASYki, UASproDronc, UASArm<sup>S10</sup>* stained for expression of DIAP1 ((F) red, (F’) grey), DCP1 ((F) blue, (F’’) grey), Wg ((G) red, (G’) grey), and pJNK ((G) blue, (G’’) grey). Disc magnification and orientation are identical in all panels. Scale bar = 25  $\mu$ m.

#### 4. Discussion

Oncogenic cooperation is a key mechanism for tumor development and progression. Cooperative interactions between oncogenic *Ras* and loss of *scrib*<sup>−</sup> (*Ras*<sup>V12</sup>,*scrib*<sup>−</sup>) have been elegantly modeled using in vivo mosaic tumor models in *Drosophila* [8,9,12,38] and multiple mammalian cancer models [59–63]. We investigated how altered signaling and cell–cell interactions promote tumorigenesis during oncogenic cooperation. Previously ectopic upregulation of a network of transcription factors, e.g., Upd, JAK-STAT, AP-1, Myc, Ftz, Ets, Irbp18, Xrp1, slow border, and Vrille, were reported to promote the growth and invasiveness of the *Ras*<sup>V12</sup>,*scrib*<sup>−</sup> tumors [64–68]. Data acquired from transcriptomics or RNA-seq have shown the presence of multiple transcription factors in the same genotype suggesting that several pathways and signals may be simultaneously active that culminate in the upregulation of several different transcription factors in tumor cells. These studies also confirm that several transcription factors are active based on the activation of their target genes. However, the potential molecular networks established remained unclear. Here we present evidence to show that a tumor cell-specific network is formed in *Ras*<sup>V12</sup>,*scrib*<sup>−/−</sup> tumors in eye imaginal discs. This network is comprised of Yki, JNK, Wg, and caspases that act to promote fitness and aggressive growth (Figures 1 and S1). Our findings from the eye discs are relevant to other epithelia, like the wing discs as the tumor-specific network, is recapitulated in the *en > Yki; scrib*<sup>−</sup> wing tumors (Figure 5).

Of these signals, JNK is very well documented as a modulator of Yki activity in the context of cell competition, compensatory proliferation, regeneration, and neoplastic tumors [12,14]. JNK is a pivotal stress-responsive kinase that promotes malignant transformation and metastasis of tumors [38,45]. JNK has also emerged as a key paracrine signal that links apoptosis to carcinogenesis [12]. In *scrib*<sup>−</sup> cells, JNK signaling suppresses Yki activity and promotes cell competition [12,69]. Concomitantly, JNK signaling causes the non-cell-autonomous propagation of Yki in the cells surrounding *scrib*<sup>−</sup> clones and promotes compensatory proliferation [12,69]. Thus, in *scrib*<sup>−</sup> clones in the wild-type background, JNK (Figure S5B) and Yki (Figure S5C,D) activities are induced in two distinct cell populations, and wild-type levels of Dronc (Figure S5E) or Wg (Figure S5F) are sufficient to support the cell competition-mediated elimination of *scrib*<sup>−</sup> cells. Work from our lab and others showed that the suppression of cell death in *scrib*<sup>−</sup> cells led to increased proliferation and the loss of differentiation, but not tumorigenesis (Figure S1A,C) [70,71]. In contrast, we found that these signaling interactions are significantly altered in *Ras*<sup>V12</sup>,*scrib*<sup>−</sup> cells, as Wg, Dronc, JNK, and Yki are all robustly upregulated (Figures 1 and S1), suggesting a non-apoptotic tumor growth-promoting role for JNK and Dronc and growth-promoting mitogenic roles for Yki and Wg. Using reporter assays for *dronc* and *wg*, we found that *Ras*<sup>V12</sup>,*scrib*<sup>−</sup> cells show increased transcription of *dronc* (Figure 1L–N) and *wg* (Figure 1O–Q), which was confirmed using qRT-PCR (Figure S2). In addition, increased JNK activity using phospho-specific JNK antibody and Yki activity by *diap1-lacZ* reporter were confirmed in the *Ras*<sup>V12</sup>,*scrib*<sup>−</sup> clones (Figure S1). These findings are consistent with reports that JNK signaling activity is converted from anti- to pro-tumor growth through the downregulation of Hippo signaling and ultimately leads to Yki activation [14,41]. Both Yki/YAP and JNK are linked to Wg signaling, as Wg is induced in a JNK-dependent manner during regenerative growth, tumorigenesis, and compensatory proliferation [51,72,73] and interacts with Yki and the Hippo pathway during organ development and tumorigenesis [74–76]. In addition, dysregulation of the Hippo, JNK, or Wg pathway is also linked to the activation of caspase-mediated apoptosis, and recently, mild caspase induction was shown to promote tumor growth [77–79]. Thus, the identification of this molecular network is significant in the context of inter-cellular interactions that promote tumor growth.

Previous studies have shown a role for the JNK and Hippo pathway in *Ras*<sup>V12</sup> *scrib*<sup>−</sup> clones [38,41]. In our study, an assessment of the roles of JNK, Yki, Dronc, and Wg in *Ras*<sup>V12</sup>,*scrib*<sup>−</sup> tumorigenesis revealed several interesting insights. First, we found that JNK, Yki, Dronc, and Wg were all required for the aggressive growth of *Ras*<sup>V12</sup>,*scrib*<sup>−</sup>-induced tumors, as the downregulation of these signals individually resulted in a significant reduction

in tumor growth (Figure 2A). Second, we observed that in the absence of tumor-promoting signals, *Ras*<sup>V12</sup>,*scrib*<sup>-</sup>-induced tumors show reduced survival and fitness (Figure 2). Third, we identified that the four tumor-promoting signals form a tumor cell-specific signaling module in which Wg acts upstream of Dronc, which, in turn, acts upstream of a JNK–Yki-mediated positive feedback signal amplification loop (Figures 3 and 4). Signal amplification of Yki and JNK activities caused by the JNK–Yki positive feedback loop plays a key role in promoting tumorigenesis in *Ras*<sup>V12</sup>,*scrib*<sup>-</sup> cells. Fourth, we confirmed that in other instances of oncogenic cooperation (*Ras*<sup>V12</sup>//*scrib*<sup>-</sup>), this signaling module can be recapitulated (Figures 5 and 6). Fifth, the upregulation of JNK and Yki in normal epithelial cells with intact polarity is not sufficient to induce this network and tumor growth (Figures 7 and S6), which is consistent with other instances of developmental interactions between Yki and JNK in polarized epithelia [80,81]. Taken together, our studies reveal that increased cellular fitness promoted by a molecular network comprising Wg, Dronc, JNK, and Yki may indeed be a mechanism co-opted for aggressive tumor growth. Furthermore, the overexpression of pathway components in the normal epithelia of wing discs revealed that the signal overactivation levels and the apical-basal polarity context are extremely important. This is because mild hyperplasia can occur by driving the individual transgenes, but robust overgrowth is not seen in cells with intact polarity. Further, for the JNK pathway, a threshold is critical, as stress-induced cell death occurs both when levels of JNK reach above or below the homeostatic levels (Figures 7 and S6).

Another possible mechanism is the differential success of cancer and neighboring normal cells in competing for survival and other extracellular signals in terms of actively internalizing or limiting the extracellular spread of critical signals. In this context, we observed steep differences in the non-cell-autonomous spread of Yki activity among *scrib*<sup>-</sup> (Figures 5 and S5C), *Ras*<sup>V12</sup> *scrib*<sup>-</sup> (Figure S1G,G'), and *en > Yki; scrib*<sup>-</sup> (Figure 5B) cells. Non-cell-autonomous Yki activity spreads to 3–5 cells in *scrib*<sup>-</sup> cells, several cells (8–10) in *en > Yki; scrib*<sup>-</sup>, and only a few cells (~2) around the *Ras*<sup>V12</sup>,*scrib*<sup>-</sup> clones. Further, cell-autonomous and non-cell-autonomous cell death is observed on the depletion of Yki (Figure 2B), suggesting that cells with impaired Yki expression are vulnerable to elimination by unidentified mechanisms. Interestingly, both cell-autonomous and non-cell-autonomous expression of Wg is seen when the components of the Wg–Dronc–JNK–Yki network are perturbed (Figure 3). Thus, limiting the extracellular spread of key signaling components like Yki or Wg may impact the growth potential of cancer cells. The mechanisms by which cancer cells limit the spread of these signals should be elucidated in future studies and may provide molecular insights about how benign and malignant tumors behave.

The biological significance of our findings is validated by other studies that show the formation of context-dependent Yki/YAP-mediated signaling loops as a bona fide mechanism for tumor growth [82,83]. YAP is not only regulated by signaling pathways like Wnt, TGFβ, and notch, but YAP can also collaborate with key cancer pathways to form transcriptional complexes that alter transcriptional programs, specifically in cancer cells [84,85]. At least three different mechanisms have been reported. First, YAP and its cognate transcription factors like TEAD control transcription by binding to promoters of target genes. Second, YAP collaborates with other transcription regulators to alter gene expression, for example, in colon cancer cell lines YAP1, β-catenin, and TBX5 transcriptional complex regulate (TCF- or TEAD-independent) target genes [86]. Third, YAP/TEAD binds distal regulatory elements to regulate the transcription of target genes [87–89]. ChIP-seq and deep-sequencing studies in cancer and normal cells showed that several YAP-binding regions also show a consensus motif for AP-1 transcriptional factors, suggesting that YAP/TEAD and AP-1 cooperatively regulate target genes representing a cross-talk between YAP and JNK signaling [88,89].

These findings are especially interesting considering our identification of the tumor-cell-specific Wg–Dronc–JNK–Yki molecular network and the JNK–Yki positive feedback signal amplification loop in the *Ras*<sup>V12</sup> *scrib*<sup>-</sup> cells. Like YAP, *Drosophila* Yki is known to regulate transcription by binding to the promoter regions of genes [90]. Similarly, Yki

can form transcriptional complexes that cooperatively alter gene expression in cancer cells, for example, Yki and the Ecdysone receptor coactivator Taiman were shown to alter the transcriptional output of Yki-inducible Taiman-dependent genes in cells with hyperactive Yki and neoplastic tumor growth [91]. Based on our data, it is possible that under conditions of oncogenic cooperation, Yki and the *Drosophila* AP-1 transcription factors may (cooperatively) bind other regulatory regions to drive altered transcriptional output in cancer cells. This conclusion is further strengthened by the finding that dFos, a component of the *Drosophila* AP-1 (*Drosophila* Jun and Fos heterodimer) transcription factor, is required for the JNK-mediated invasiveness of *Ras*<sup>V12</sup>,*scrib*<sup>-</sup> tumors [44,66]. In summary, cancer cells may establish specific molecular networks that promote tumor growth and metastasis, and it may be critical to understand these interactions to understand how oncogenic pathways are activated.

## 5. Conclusions

Our data are significant in light of emerging data from cancer genome studies that revealed that somatic mutations accrued by precancerous cells essentially activate hallmark cancer pathways that converge on a small number of protein complexes and signaling cascades [6]. Our genetic analyses indicate the hierarchy of one such signaling interaction, with Wg acting upstream of Dronc, JNK, and Yki, and in the future, it will be interesting to identify the molecular mechanisms underlying the establishment and regulation of this module. These approaches can also unveil targets for the modulation of the tumor and provide insights into the biomechanics of tumor progression. Our approach of modeling altered signaling interactions in a genetically tractable model is a powerful way to reconstruct key biologically meaningful changes in signaling pathways in cancer cells and provides a functional framework to study the changes in signaling pathway interactions that will generate new insights on mechanisms that promote tumor growth and progression.

**Supplementary Materials:** The following supporting information can be downloaded at: <https://www.mdpi.com/article/10.3390/cancers16091768/s1>, Figure S1 (related to Figure 1): Growth of *scrib* mutant clones and the role of Yki and JNK signaling, Figure S2 (related to Figure 1): Upregulation of *wg* and *dronc* expression in *Ras*<sup>V12</sup> *scrib*<sup>-</sup> clones, Figure S3 (related to Figure 2): Assessment of cell survival in *Ras*<sup>V12</sup> *scrib*<sup>-</sup> clones, Figure S4 (related to Figure 2): Effects of downregulation of network components in wild-type cells, Figure S5 (related to Figure 5): Effects of loss of *scrib* on the molecular network, Figure S6 (related to Figure 7): Activation of individual network components in polarity intact cells cause mild effects in promoting *Ras*<sup>V12</sup> *scrib*<sup>-</sup> clones.

**Author Contributions:** Conceptualization, M.K.-S. and A.S.; methodology, M.K.-S. and I.W.; formal analysis, I.W., K.G., A.R. and M.K.-S.; investigation, I.W., M.K.-S. and A.S.; resources, A.S. and M.K.-S.; writing, original draft preparation, I.W. and M.K.-S.; writing, review and editing, I.W., A.R., A.S. and M.K.-S.; supervision, M.K.-S.; project administration, M.K.-S.; funding acquisition, M.K.-S. and A.S. All authors have read and agreed to the published version of the manuscript.

**Funding:** This research was funded by start-up research funds from the University of Dayton and STEM Catalyst Grant to M.K.-S., National Institutes of Health grant 1RO1EY032959-01 (PI: A. Singh and M. Kango-Singh); the start-up funds and STEM Catalyst Grant from University of Dayton to A.S., I.W., K.G. and A.R. were supported by Graduate Teaching Assistantships and Graduate Student Summer Fellowships at the University of Dayton.

**Institutional Review Board Statement:** Not applicable.

**Informed Consent Statement:** Not applicable.

**Data Availability Statement:** Data is maintained within this article.

**Acknowledgments:** We would like to thank A. Bergmann, G. Halder, B. Hay, K. D. Irvine, H.D. Ryoo, and Tin Tin Su and the Bloomington *Drosophila* Stock Center, the *Drosophila* Genetics Resource Center (Japan), and the Developmental Studies Hybridoma Bank for flies and antibodies, as well as the members of the Kango-Singh and Singh Labs for comments and suggestions on the manuscript.

I.W., K.G., and A.R. acknowledge the Graduate School at the University of Dayton for the Graduate Student Summer Fellowships.

**Conflicts of Interest:** The authors declare no conflict of interest.

## References

- Blum, A.; Wang, P.; Zenklusen, J.C. SnapShot: TCGA-Analyzed Tumors. *Cell* **2018**, *173*, 530. [[CrossRef](#)] [[PubMed](#)]
- Mertins, P.; Tang, L.C.; Krug, K.; Clark, D.J.; Gritsenko, M.A.; Chen, L.; Clauser, K.R.; Clauss, T.R.; Shah, P.; Gillette, M.A.; et al. Reproducible workflow for multiplexed deep-scale proteome and phosphoproteome analysis of tumor tissues by liquid chromatography–mass spectrometry. *Nat. Protoc.* **2018**, *13*, 1632–1661. [[CrossRef](#)] [[PubMed](#)]
- Sanchez-Vega, F.; Mina, M.; Armenia, J.; Chatila, W.K.; Luna, A.; La, K.C.; Dimitriadoy, S.; Liu, D.L.; Kantheti, H.S.; Saghafeina, S.; et al. Oncogenic Signaling Pathways in The Cancer Genome Atlas. *Cell* **2018**, *173*, 321–337.e10. [[CrossRef](#)] [[PubMed](#)]
- Weinstein, J.N.; Collisson, E.A.; Mills, G.B.; Shaw, K.R.M.; Ozenberger, B.A.; Ellrott, K.; Shmulevich, I.; Sander, C.; Stuart, J.M. The Cancer Genome Atlas Research Network, The Cancer Genome Atlas Pan-Cancer analysis project. *Nat. Genet.* **2013**, *45*, 1113–1120. [[CrossRef](#)] [[PubMed](#)]
- De Vreede, G.; Gerlach, S.U.; Bilder, D. Epithelial monitoring through ligand-receptor segregation ensures malignant cell elimination. *Science* **2022**, *376*, 297–301. [[CrossRef](#)]
- Vogelstein, B.; Papadopoulos, N.; Velculescu, V.E.; Zhou, S.; Diaz, L.A.; Kinzler, K.W. Cancer Genome Landscapes. *Science* **2013**, *339*, 1546–1558. [[CrossRef](#)] [[PubMed](#)]
- Torkamani, A.; Verkhivker, G.; Schork, N.J. Cancer driver mutations in protein kinase genes. *Cancer Lett.* **2009**, *281*, 117–127. [[CrossRef](#)] [[PubMed](#)]
- Pagliarini, R.A.; Xu, T. A Genetic Screen in *Drosophila* for Metastatic Behavior. *Science* **2003**, *302*, 1227–1231. [[CrossRef](#)]
- Brumby, A.M. Scribble mutants cooperate with oncogenic Ras or Notch to cause neoplastic overgrowth in *Drosophila*. *EMBO J.* **2003**, *22*, 5769–5779. [[CrossRef](#)]
- Wu, M.; Pastor-Pareja, J.C.; Xu, T. Interaction between RasV12 and scribbled clones induces tumour growth and invasion. *Nature* **2010**, *463*, 545–548. [[CrossRef](#)]
- Dillard, C.; Reis, J.G.T.; Rusten, T.E. RasV12; scrib<sup>-/-</sup> – Tumors: A Cooperative Oncogenesis Model Fueled by Tumor/Host Interactions. *Int. J. Mol. Sci.* **2021**, *22*, 8873. [[CrossRef](#)] [[PubMed](#)]
- Chen, C.-L.; Schroeder, M.C.; Kango-Singh, M.; Tao, C.; Halder, G. Tumor suppression by cell competition through regulation of the Hippo pathway. *Proc. Natl. Acad. Sci. USA* **2012**, *109*, 484–489. [[CrossRef](#)]
- Sun, G.; Irvine, K.D. Ajuba Family Proteins Link JNK to Hippo Signaling. *Sci. Signal.* **2013**, *6*, ra81. [[CrossRef](#)] [[PubMed](#)]
- Sun, G.; Irvine, K.D. Regulation of Hippo signaling by Jun kinase signaling during compensatory cell proliferation and regeneration, and in neoplastic tumors. *Dev. Biol.* **2011**, *350*, 139–151. [[CrossRef](#)] [[PubMed](#)]
- Gerlach, S.U.; Eichenlaub, T.; Herranz, H. Yorkie and JNK Control Tumorigenesis in *Drosophila* Cells with Cytokinesis Failure. *Cell Rep.* **2018**, *23*, 1491–1503. [[CrossRef](#)] [[PubMed](#)]
- Ma, X.; Wang, H.; Ji, J.; Xu, W.; Sun, Y.; Li, W.; Zhang, X.; Chen, J.; Xue, L. Hippo signaling promotes JNK-dependent cell migration. *Proc. Natl. Acad. Sci. USA* **2017**, *114*, 1934–1939. [[CrossRef](#)] [[PubMed](#)]
- Bejsovec, A. Wingless Signaling: A Genetic Journey from Morphogenesis to Metastasis. *Genetics* **2018**, *208*, 1311–1336. [[CrossRef](#)]
- Irvine, K.D.; Harvey, K.F. Control of Organ Growth by Patterning and Hippo Signaling in *Drosophila*. *Cold Spring Harb. Perspect. Biol.* **2015**, *7*, a019224. [[CrossRef](#)]
- Kockel, L.; Homsy, J.G.; Bohmann, D. *Drosophila* AP-1: Lessons from an invertebrate. *Oncogene* **2001**, *20*, 2347–2364. [[CrossRef](#)]
- Shalini, S.; Dorstyn, L.; Dawar, S.; Kumar, S. Old, new and emerging functions of caspases. *Cell Death Differ.* **2015**, *22*, 526–539. [[CrossRef](#)]
- Suzanne, M.; Steller, H. Shaping organisms with apoptosis. *Cell Death Differ.* **2013**, *20*, 669–675. [[CrossRef](#)] [[PubMed](#)]
- Eichenlaub, T.; Cohen, S.M.; Herranz, H. Cell competition drives the formation of metastatic tumors in a *drosophila* model of epithelial tumor formation. *Curr. Biol.* **2016**, *26*, 419–427. [[CrossRef](#)] [[PubMed](#)]
- Morata, G.; Ballesteros-Arias, L. Cell competition, apoptosis and tumour development. *Int. J. Dev. Biol.* **2015**, *59*, 79–86. [[CrossRef](#)] [[PubMed](#)]
- Baillon, L.; Basler, K. Reflections on cell competition. *Semin. Cell Dev. Biol.* **2014**, *32*, 137–144. [[CrossRef](#)] [[PubMed](#)]
- Fan, Y.; Bergmann, A. Apoptosis-induced compensatory proliferation. The Cell is dead. Long live the Cell! *Trends Cell Biol.* **2008**, *18*, 467–473. [[CrossRef](#)]
- Hajra, K.M.; Liu, J.R. Apoptosome dysfunction in human cancer. *Apoptosis* **2004**, *9*, 691–704. [[CrossRef](#)] [[PubMed](#)]
- Wells, B.S.; Yoshida, E.; Johnston, L.A. Compensatory Proliferation in *Drosophila* Imaginal Discs Requires Dronc-Dependent p53 Activity. *Curr. Biol.* **2006**, *16*, 1606–1615. [[CrossRef](#)] [[PubMed](#)]
- Huh, J.R.; Guo, M.; Hay, B.A. Compensatory proliferation induced by cell death in the *Drosophila* wing disc requires activity of the apical cell death caspase dronc in a nonapoptotic role. *Curr. Biol.* **2004**, *14*, 1262–1266. [[CrossRef](#)] [[PubMed](#)]
- Bilder, D.; Perrimon, N. Localization of apical epithelial determinants by the basolateral PDZ protein Scribble. *Nature* **2000**, *403*, 676–680. [[CrossRef](#)]

30. Cakouros, D.; Daish, T.J.; Kumar, S. Ecdysone receptor directly binds the promoter of the *Drosophila* caspase dronc, regulating its expression in specific tissues. *J. Cell Biol.* **2004**, *165*, 631–640. [[CrossRef](#)]
31. Boedigheimer, M.; Bryant, P.; Laughon, A. Expanded, a negative regulator of cell proliferation in *Drosophila*, shows homology to the NF2 tumor suppressor. *Mech. Dev.* **1993**, *44*, 83–84. [[CrossRef](#)] [[PubMed](#)]
32. Ma, C.; Moses, K. *Wingless* and *patched* are negative regulators of the morphogenetic furrow and can affect tissue polarity in the developing *Drosophila* compound eye. *Development* **1995**, *121*, 2279–2289. [[CrossRef](#)] [[PubMed](#)]
33. Ito, K.; Awano, W.; Suzuki, K.; Hiromi, Y.; Yamamoto, D. The *Drosophila* mushroom body is a quadruple structure of clonal units each of which contains a virtually identical set of neurones and glial cells. *Development* **1997**, *124*, 761–771. [[CrossRef](#)] [[PubMed](#)]
34. Zhang, L.; Ren, F.; Zhang, Q.; Chen, Y.; Wang, B.; Jiang, J. The TEAD/TEF family of transcription factor Scalloped mediates Hippo signaling in organ size control. *Dev. Cell* **2008**, *14*, 377–387. [[CrossRef](#)] [[PubMed](#)]
35. Treier, M.; Bohmann, D.; Mlodzik, M. JUN cooperates with the ETS domain protein pointed to induce photoreceptor R7 fate in the *Drosophila* eye. *Cell* **1995**, *83*, 753–760. [[CrossRef](#)]
36. Huang, J.; Wu, S.; Barrera, J.; Matthews, K.; Pan, D. The Hippo Signaling Pathway Coordinately Regulates Cell Proliferation and Apoptosis by Inactivating Yorkie, the *Drosophila* Homolog of YAP. *Cell* **2005**, *122*, 421–434. [[CrossRef](#)] [[PubMed](#)]
37. Kango-Singh, M.; Nolo, R.; Tao, C.; Verstreken, P.; Hiesinger, P.R.; Bellen, H.J.; Halder, G. Shar-pei mediates cell proliferation arrest during imaginal disc growth in *Drosophila*. *Development* **2002**, *129*, 5719–5730. [[CrossRef](#)]
38. Igaki, T.; Pagliarini, R.A.; Xu, T. Loss of Cell Polarity Drives Tumor Growth and Invasion through JNK Activation in *Drosophila*. *Curr. Biol.* **2006**, *16*, 1139–1146. [[CrossRef](#)]
39. Hay, B.A.; Wolff, T.; Rubin, G.M. Expression of baculovirus P35 prevents cell death in *Drosophila*. *Development* **1994**, *120*, 2121–2129. [[CrossRef](#)]
40. Vincent, J.-P.; Fletcher, A.G.; Baena-Lopez, L.A. Mechanisms and mechanics of cell competition in epithelia. *Nat. Rev. Mol. Cell Biol.* **2013**, *14*, 581–591. [[CrossRef](#)]
41. Enomoto, M.; Kizawa, D.; Ohsawa, S.; Igaki, T. JNK signaling is converted from anti- to pro-tumor pathway by Ras-mediated switch of Warts activity. *Dev. Biol.* **2015**, *403*, 162–171. [[CrossRef](#)]
42. Snigdha, K.; Singh, A.; Kango-Singh, M. Yorkie-Cactus ( $\text{I}\kappa\text{B}\alpha$ )-JNK axis promotes tumor growth and progression in *Drosophila*. *Oncogene* **2021**, *40*, 4124–4136. [[CrossRef](#)]
43. Ziosi, M.; Baena-López, L.A.; Grifoni, D.; Froidi, F.; Pession, A.; Garoia, F.; Trotta, V.; Bellosta, P.; Cavicchi, S.; Pession, A. dMyc functions downstream of yorkie to promote the supercompetitive behavior of hippo pathway mutant Cells. *PLoS Genet.* **2010**, *6*, e1001140. [[CrossRef](#)] [[PubMed](#)]
44. Uhlirova, M.; Bohmann, D. JNK- and Fos-regulated Mmp1 expression cooperates with Ras to induce invasive tumors in *Drosophila*. *EMBO J.* **2006**, *25*, 5294–5304. [[CrossRef](#)] [[PubMed](#)]
45. Doggett, K.; Grusche, F.A.; Richardson, H.E.; Brumby, A.M. Loss of the *Drosophila* cell polarity regulator Scribbled promotes epithelial tissue overgrowth and cooperation with oncogenic Ras-Raf through impaired Hippo pathway signaling. *BMC Dev. Biol.* **2011**, *11*, 57. [[CrossRef](#)]
46. Igaki, T.; Pastor-Pareja, J.C.; Aonuma, H.; Miura, M.; Xu, T. Intrinsic Tumor Suppression and Epithelial Maintenance by Endocytic Activation of Eiger/TNF Signaling in *Drosophila*. *Dev. Cell* **2009**, *16*, 458–465. [[CrossRef](#)]
47. Garcia-Arias, J.M.; Pinal, N.; Cristobal-Vargas, S.; Estella, C.; Morata, G. Lack of apoptosis leads to cellular senescence and tumorigenesis in *Drosophila* epithelial cells. *Cell Death Discov.* **2023**, *9*, 281. [[CrossRef](#)] [[PubMed](#)]
48. La Marca, J.E.; Richardson, H.E. Two-Faced: Roles of JNK Signalling During Tumourigenesis in the *Drosophila* Model. *Front. Cell Dev. Biol.* **2020**, *8*, 42. [[CrossRef](#)]
49. Senoo-Matsuda, N.; Johnston, L.A. Soluble factors mediate competitive and cooperative interactions between cells expressing different levels of *Drosophila* Myc. *Proc. Natl. Acad. Sci. USA* **2007**, *104*, 18543–18548. [[CrossRef](#)]
50. Fan, Y.; Bergmann, A. Distinct mechanisms of apoptosis-induced compensatory proliferation in proliferating and differentiating tissues in the *Drosophila* eye. *Dev. Cell* **2008**, *14*, 399–410. [[CrossRef](#)]
51. Ryoo, H.D.; Gorenc, T.; Steller, H. Apoptotic Cells Can Induce Compensatory Cell Proliferation through the JNK and the Wingless Signaling Pathways. *Dev. Cell* **2004**, *7*, 491–501. [[CrossRef](#)] [[PubMed](#)]
52. Verghese, S.; Bedi, S.; Kango-Singh, M. Hippo signalling controls Dronc activity to regulate organ size in *Drosophila*. *Cell Death Differ.* **2012**, *19*, 1664–1676. [[CrossRef](#)]
53. Cho, E.; Feng, Y.; Rauskolb, C.; Maitra, S.; Fehon, R.; Irvine, K.D. Delineation of a Fat tumor suppressor pathway. *Nat. Genet.* **2006**, *38*, 1142–1150. [[CrossRef](#)] [[PubMed](#)]
54. Hazelett, D.J.; Bourouis, M.; Walldorf, U.; Treisman, J.E. *Decapentaplegic* and *wingless* are regulated by *eyes absent* and *eyegone* and interact to direct the pattern of retinal differentiation in the eye disc. *Development* **1998**, *125*, 3741–3751. [[CrossRef](#)] [[PubMed](#)]
55. Wang, S.L.; Hawkins, C.J.; Yoo, S.J.; Müller, H.-A.J.; Hay, B.A. The *Drosophila* Caspase Inhibitor DIAP1 Is Essential for Cell Survival and Is Negatively Regulated by HID. *Cell* **1999**, *98*, 453–463. [[CrossRef](#)] [[PubMed](#)]
56. Ingham, P.W.; Hidalgo, A. Regulation of *wingless* transcription in the *Drosophila* embryo. *Development* **1993**, *117*, 283–291. [[CrossRef](#)] [[PubMed](#)]
57. Yoffe, K.B.; Manoukian, A.S.; Wilder, E.L.; Brand, A.H.; Perrimon, N. Evidence for engrailed-Independent wingless Autoregulation in *Drosophila*. *Dev. Biol.* **1995**, *170*, 636–650. [[CrossRef](#)] [[PubMed](#)]

58. Manoukian, A.S.; Yoffe, K.B.; Wilder, E.L.; Perrimon, N. The *porcupine* gene is required for *wingless* autoregulation in *Drosophila*. *Development* **1995**, *121*, 4037–4044. [[CrossRef](#)] [[PubMed](#)]
59. Dow, L.E.; Elsum, I.A.; King, C.L.; Kinross, K.M.; Richardson, H.E.; Humbert, P.O. Loss of human Scribble cooperates with H-Ras to promote cell invasion through deregulation of MAPK signalling. *Oncogene* **2008**, *27*, 5988–6001. [[CrossRef](#)]
60. Gödde, N.J.; Pearson, H.B.; Smith, L.K.; Humbert, P.O. Dissecting the role of polarity regulators in cancer through the use of mouse models. *Exp. Cell Res.* **2014**, *328*, 249–257. [[CrossRef](#)]
61. Pearson, H.B.; McGlenn, E.; Pheesse, T.J.; Schlüter, H.; Srikumar, A.; Gödde, N.J.; Woelwer, C.B.; Ryan, A.; Phillips, W.A.; Ernst, M.; et al. The polarity protein Scrib mediates epidermal development and exerts a tumor suppressive function during skin carcinogenesis. *Mol. Cancer* **2015**, *14*, 169. [[CrossRef](#)] [[PubMed](#)]
62. Elsum, I.; Yates, L.; Humbert, P.O.; Richardson, H.E. The Scribble–Dlg–Lgl polarity module in development and cancer: From flies to man. *Essays Biochem.* **2012**, *53*, 141–168. [[CrossRef](#)] [[PubMed](#)]
63. Adachi, Y.; Kimura, R.; Hirade, K.; Yanase, S.; Nishioka, Y.; Kasuga, N.; Yamaguchi, R.; Ebi, H. Scribble mis-localization induces adaptive resistance to KRAS G12C inhibitors through feedback activation of MAPK signaling mediated by YAP-induced MRAS. *Nat. Cancer* **2023**, *4*, 829–843. [[CrossRef](#)] [[PubMed](#)]
64. Floc'Hlay, S.; Balaji, R.; Stanković, D.; Christiaens, V.M.; González-Blas, C.B.; De Winter, S.; Hulselmans, G.J.; De Waegeneer, M.; Quan, X.; Koldere, D.; et al. Shared enhancer gene regulatory networks between wound and oncogenic programs. *eLife* **2023**, *12*, e81173. [[CrossRef](#)]
65. Atkins, M.; Potier, D.; Romanelli, L.; Jacobs, J.; Mach, J.; Hamaratoglu, F.; Aerts, S.; Halder, G. An Ectopic Network of Transcription Factors Regulated by Hippo Signaling Drives Growth and Invasion of a Malignant Tumor Model. *Curr. Biol.* **2016**, *26*, 2101–2113. [[CrossRef](#)] [[PubMed](#)]
66. Külshammer, E.; Mundorf, J.; Kilinc, M.; Frommolt, P.; Wagle, P.; Uhlirva, M. Interplay among transcription factors Ets21c, Fos and Ftz-F1 drives JNK-mediated tumor malignancy. *Dis. Models Mech.* **2015**, *8*, dmm.020719. [[CrossRef](#)] [[PubMed](#)]
67. Bunker, B.D.; Nellimoottil, T.T.; Boileau, R.M.; Classen, A.K.; Bilder, D. The transcriptional response to tumorigenic polarity loss in *Drosophila*. *eLife* **2015**, *4*, e03189. [[CrossRef](#)] [[PubMed](#)]
68. Ji, T.; Zhang, L.; Deng, M.; Huang, S.; Wang, Y.; Pham, T.T.; Smith, A.A.; Sridhar, V.; Cabernard, C.; Wang, J.; et al. Dynamic MAPK signaling activity underlies a transition from growth arrest to proliferation in *Drosophila scribble* mutant tumors. *Dis. Models Mech.* **2019**, *12*, dmm.040147. [[CrossRef](#)] [[PubMed](#)]
69. Verghese, S.; Waghmare, I.; Kwon, H.; Hanes, K.; Kango-Singh, M. Scribble Acts in the *Drosophila* Fat-Hippo Pathway to Regulate Warts Activity. *PLoS ONE* **2012**, *7*, e47173. [[CrossRef](#)]
70. Waghmare, I.; Kango-Singh, M. Loss of Cell Adhesion Increases Tumorigenic Potential of Polarity Deficient Scribble Mutant Cells. *PLoS ONE* **2016**, *11*, e0158081. [[CrossRef](#)]
71. Pérez, E.; Lindblad, J.L.; Bergmann, A. Tumor-promoting function of apoptotic caspases by an amplification loop involving ROS, macrophages and JNK in *Drosophila*. *eLife* **2017**, *6*, e26747. [[CrossRef](#)]
72. Pérez-Garijo, A.; Martín, F.A.; Morata, G. Caspase inhibition during apoptosis causes abnormal signalling and developmental aberrations in *Drosophila*. *Development* **2004**, *131*, 5591–5598. [[CrossRef](#)] [[PubMed](#)]
73. Smith-Bolton, R.K.; Worley, M.I.; Kanda, H.; Hariharan, I.K. Regenerative Growth in *Drosophila* Imaginal Discs Is Regulated by Wingless and Myc. *Dev. Cell* **2009**, *16*, 797–809. [[CrossRef](#)] [[PubMed](#)]
74. Zecca, M.; Struhl, G. A Feed-Forward Circuit Linking Wingless, Fat-Dachsous Signaling, and the Warts-Hippo Pathway to *Drosophila* Wing Growth. *PLoS Biol.* **2010**, *8*, e1000386. [[CrossRef](#)] [[PubMed](#)]
75. Konsavage, W.M.; Yochum, G.S. Intersection of Hippo/YAP and Wnt/ $\beta$ -catenin signaling pathways. *Acta Biochim. Biophys. Sin.* **2013**, *45*, 71–79. [[CrossRef](#)] [[PubMed](#)]
76. Wittkorn, E.; Sarkar, A.; Garcia, K.; Kango-Singh, M.; Singh, A. The Hippo pathway effector Yki downregulates Wg signaling to promote retinal differentiation in the *Drosophila* eye. *Development* **2015**, *142*, 2002–2013. [[CrossRef](#)]
77. Zimmerman, M.A.; Huang, Q.; Li, F.; Liu, X.; Li, C.-Y. Cell Death–Stimulated Cell Proliferation: A Tissue Regeneration Mechanism Usurped by Tumors During Radiotherapy. *Semin. Radiat. Oncol.* **2013**, *23*, 288–295. [[CrossRef](#)] [[PubMed](#)]
78. Huang, Q.; Li, F.; Liu, X.; Li, W.; Shi, W.; Liu, F.-F.; O'Sullivan, B.; He, Z.; Peng, Y.; Tan, A.-C.; et al. Caspase 3–mediated stimulation of tumor cell repopulation during cancer radiotherapy. *Nat. Med.* **2011**, *17*, 860–866. [[CrossRef](#)]
79. Xu, D.C.; Wang, L.; Yamada, K.M.; Baena-Lopez, L.A. Non-apoptotic activation of *Drosophila* caspase-2/9 modulates JNK signaling, the tumor microenvironment, and growth of wound-like tumors. *Cell Rep.* **2022**, *39*, 110718. [[CrossRef](#)]
80. Liu, S.; Sun, J.; Wang, D.; Pflugfelder, G.O.; Shen, J. Fold formation at the compartment boundary of *Drosophila* wing requires Yki signaling to suppress JNK dependent apoptosis. *Sci. Rep.* **2016**, *6*, 38003. [[CrossRef](#)]
81. Ma, X.; Chen, Y.; Xu, W.; Wu, N.; Li, M.; Cao, Y.; Wu, S.; Li, Q.; Xue, L. Impaired Hippo signaling promotes Rho1–JNK-dependent growth. *Proc. Natl. Acad. Sci. USA* **2015**, *112*, 1065–1070. [[CrossRef](#)] [[PubMed](#)]
82. Calvo, F.; Ege, N.; Grande-Garcia, A.; Hooper, S.; Jenkins, R.P.; Chaudhry, S.I.; Harrington, K.; Williamson, P.; Moeendarbary, E.; Charras, G.; et al. Mechanotransduction and YAP-dependent matrix remodelling is required for the generation and maintenance of cancer-associated fibroblasts. *Nat. Cell Biol.* **2013**, *15*, 637–646. [[CrossRef](#)] [[PubMed](#)]
83. Hong, X.; Nguyen, H.T.; Chen, Q.; Zhang, R.; Hagman, Z.; Voorhoeve, P.M.; Cohen, S.M. Opposing activities of the R as and Hippo pathways converge on regulation of YAP protein turnover. *EMBO J.* **2014**, *33*, 2447–2457. [[CrossRef](#)] [[PubMed](#)]

84. Barry, E.R.; Camargo, F.D. The Hippo superhighway: Signaling crossroads converging on the Hippo/Yap pathway in stem cells and development. *Curr. Opin. Cell Biol.* **2013**, *25*, 247–253. [[CrossRef](#)]
85. Meng, Z.; Moroishi, T.; Guan, K.-L. Mechanisms of Hippo pathway regulation. *Genes Dev.* **2016**, *30*, 1–17. [[CrossRef](#)] [[PubMed](#)]
86. Rosenbluh, J.; Nijhawan, D.; Cox, A.G.; Li, X.; Neal, J.T.; Schafer, E.J.; Zack, T.I.; Wang, X.; Tsherniak, A.; Schinzel, A.C.; et al.  $\beta$ -Catenin-Driven Cancers Require a YAP1 Transcriptional Complex for Survival and Tumorigenesis. *Cell* **2012**, *151*, 1457–1473. [[CrossRef](#)] [[PubMed](#)]
87. Galli, G.G.; Carrara, M.; Yuan, W.-C.; Valdes-Quezada, C.; Gurung, B.; Pepe-Mooney, B.; Zhang, T.; Geeven, G.; Gray, N.S.; de Laat, W.; et al. YAP Drives Growth by Controlling Transcriptional Pause Release from Dynamic Enhancers. *Mol. Cell* **2015**, *60*, 328–337. [[CrossRef](#)] [[PubMed](#)]
88. Stein, C.; Bardet, A.F.; Roma, G.; Bergling, S.; Clay, I.; Ruchti, A.; Agarinis, C.; Schmelzle, T.; Bouwmeester, T.; Schübeler, D.; et al. YAP1 Exerts Its Transcriptional Control via TEAD-Mediated Activation of Enhancers. *PLoS Genet.* **2015**, *11*, e1005465. [[CrossRef](#)]
89. Zanconato, F.; Forcato, M.; Battilana, G.; Azzolin, L.; Quaranta, E.; Bodega, B.; Rosato, A.; Bicciato, S.; Cordenonsi, M.; Piccolo, S. Genome-wide association between YAP/TAZ/TEAD and AP-1 at enhancers drives oncogenic growth. *Nat. Cell Biol.* **2015**, *17*, 1218–1227. [[CrossRef](#)]
90. Oh, H.; Slattery, M.; Ma, L.; Crofts, A.; White, K.P.; Mann, R.S.; Irvine, K.D. Genome-wide Association of Yorkie with Chromatin and Chromatin-Remodeling Complexes. *Cell Rep.* **2013**, *3*, 309–318. [[CrossRef](#)]
91. Zhang, C.; Robinson, B.S.; Xu, W.; Yang, L.; Yao, B.; Zhao, H.; Byun, P.K.; Jin, P.; Veraksa, A.; Moberg, K.H. The Ecdysone Receptor Coactivator Taiman Links Yorkie to Transcriptional Control of Germline Stem Cell Factors in Somatic Tissue. *Dev. Cell* **2015**, *34*, 168–180. [[CrossRef](#)] [[PubMed](#)]

**Disclaimer/Publisher’s Note:** The statements, opinions and data contained in all publications are solely those of the individual author(s) and contributor(s) and not of MDPI and/or the editor(s). MDPI and/or the editor(s) disclaim responsibility for any injury to people or property resulting from any ideas, methods, instructions or products referred to in the content.